Received: 18 January 2019 | Accepted: 19 August 2019

DOI: 10.1111/1365-2745.13276

Journal of Ecology | BRITISH ECOLOGICAL SOCIETY

RESEARCH ARTICLE

Plant economic strategies of grassland species control soil carbon dynamics through rhizodeposition

Ludovic Henneron[1,2] | Camille Cros[1] | Catherine Picon-Cochard[1] | Vida Rahimian[1] | Sébastien Fontaine[1]

[1]UMR Ecosystème Prairial, INRA, Clermont-Ferrand, France

[2]Department of Forest Ecology and Management, Swedish University of Agricultural Sciences, Umeå, Sweden

Correspondence
Ludovic Henneron
Email: ludovic_henneron@hotmail.com

Funding information
French National Research Agency, Grant/Award Number: ANR 14-CE01-0004 and ANR-11-LABX-0002-01

Handling Editor: Franciska de Vries

Abstract

1. The plant economics spectrum is increasingly recognized as a major determinant of plant species effects on terrestrial ecosystem functioning related to carbon cycling. However, the role of plant economic strategies in the effects of living root activity on soil organic carbon (SOC) dynamics through rhizodeposition remains unexplored, despite SOC being the largest terrestrial carbon pool.
2. Using a continuous ^{13}C-labelling method allowing partitioning of plant and soil sources to carbon fluxes and pools, we studied here the linkages between plant economic strategies and SOC cycling processes in a 'common garden' greenhouse experiment. It includes a panel of 12 grassland species selected along a gradient of economic traits and belonging to three functionnal groups (C3 grasses, forbs and legumes).
3. All species induced an acceleration of native SOC mineralization but this rhizosphere priming effect (RPE) substantially differed across species and varied elevenfold by the end of the experiment (from +26% to +295% relative to unplanted soil). Interspecific variation in RPE was primarily linked to plant photosynthetic activity associated to species economic strategies of light and CO_2 resource acquisition and processing. Fast-growing acquisitive species, such as legumes, featured large RPE, in relation with their high canopy photosynthesis coupled to high leaf photosynthetic capacity and large net primary productivity allocated above-ground. This large RPE was further associated with high root metabolic activity, rhizodeposition and soil microbial activity. In contrast, fine-root growth and economic traits related to soil resource foraging ability were poor predictors of RPE.
4. The formation of new root-derived SOC varied nine-fold across species and was similarly positively related to the net primary productivity allocated above-ground. Fast-growing acquisitive species with a high photosynthetic activity induced a disproportionately large RPE relative to SOC formation.
5. *Synthesis*. Overall, our study demonstrates that rhizodeposition is a major mechanism through which plant economic strategies of grassland species control soil

carbon dynamics. Acquisitive versus conservative species were associated with high versus low rates of photosynthesis and rhizodeposition, in turn leading to fast versus slow SOC turnover. This emphasizes the importance of considering rhizosphere processes for understanding plant species effects on soil biogeochemistry.

KEYWORDS
decomposition, ecosystem functioning, leaf and root traits, photosynthesis, plant economics spectrum, plant–soil (below-ground) interactions, rhizosphere priming effect, rhizosphere processes

1 | INTRODUCTION

Adopting a trait-based approach is increasingly emphasized as a promising avenue to improve our understanding of the effects of plant communities on ecosystem processes (Diaz & Cabido, 2001). Among the multiple dimensions of plant adaptation to their environment, the plant economics spectrum (PES) has been identified as a fundamental axis of resource acquisition and processing strategies ranging from fast-growing acquisitive to slow-growing conservative species (Reich, 2014). Acquisitive versus conservative strategies have been found to be associated with fast versus slow rates of carbon (C) cycling processes, such as plant photosynthesis and primary productivity (Garnier et al., 2004; Wright et al., 2004), as well as litter decomposition (Cornwell et al., 2008; Freschet, Aerts, & Cornelissen, 2012). However, the importance of the PES for soil organic carbon (SOC) cycling and long-term sequestration remains poorly understood (De Deyn, Cornelissen, & Bardgett, 2008; Orwin et al., 2010), even though SOC represents the largest terrestrial C pool (Schlesinger & Bernhardt, 2013). Indeed, the commonly held view that litter recalcitrance explains SOC decomposition has been challenged, and the controlling factors of SOC dynamics might be fundamentally different in comparison to those of litter decomposition (Cotrufo, Wallenstein, Boot, Denef, & Paul, 2013; Schmidt et al., 2011).

An important mechanism by which plants influence SOC dynamics is the allocation of photosynthate-C to soil by their living roots (Farrar, Hawes, Jones, & Lindow, 2003; Jones, Hodge, & Kuzyakov, 2004; Pausch & Kuzyakov, 2018). Rhizodeposition and associated rhizosphere processes are now widely recognized as major components of terrestrial ecosystem C cycling (Finzi et al., 2015; Högberg & Read, 2006). Root exudation and death lead to the formation of new root-derived SOC (Dijkstra & Cheng, 2007; Sokol, Kuebbing, Karlsen-Ayala, & Bradford, 2018). It has also been found to commonly induce an acceleration of native SOC mineralization by destabilizing mineral-organic associations (Keiluweit et al., 2015) and stimulating microbial activity and exoenzyme production (Cheng et al., 2014; Kuzyakov, 2002), a phenomenon termed the rhizosphere priming effect (RPE). A better understanding of these rhizosphere processes governing SOC dynamics is critical for predicting biospheric feedbacks to the global C cycle and climate change (Heimann & Reichstein, 2008). However, our knowledge of plant species effects on SOC cycling through rhizodeposition is still very limited, despite important shifts in vegetation composition to be expected worldwide with global change (Nolan et al., 2018).

Plant species identity has been identified as an important factor affecting rhizodeposition (Jones, Nguyen, & Finlay, 2009) and the rhizosphere priming (Cheng et al., 2014). However, previous studies were typically limited to a small species pool (Cheng, Johnson, & Fu, 2003; Dijkstra & Cheng, 2007; Wang, Tang, Severi, Butterly, & Baldock, 2016; Yin, Dijkstra Feike, Wang, Zhu, & Cheng, 2018), and the ecophysiological mechanisms involved remain elusive. Canopy photosynthetic activity supplying labile C to the rhizosphere has been suggested to be tightly coupled with soil microbial activity and SOC mineralization (Bardgett, Bowman, Kaufmann, & Schmidt, 2005; Kuzyakov & Gavrichkova, 2010). Leaf economic traits could hence be strongly related to rhizosphere priming, with higher RPE for acquisitive species with larger canopy area and photosynthetic capacity than conservative species (Wright et al., 2004). Fine-root economic traits related to root system activity and architecture could also be important by affecting rhizodeposition supply and spatial distribution (Bardgett, Mommer, & Vries, 2014; Laliberté, 2017; Roumet et al., 2016). For instance, it has been proposed that acquisitive species featuring fine and densely branched root systems with high foraging ability could promote larger RPE by increasing rhizospheric soil volume (Cheng et al., 2014; De Deyn et al., 2008; Kuzyakov, 2002; Personeni & Loiseau, 2004). More globally, plant growth rate and phenology can affect the RPE, with fast-growing species inducing larger RPE, earlier in the growing season, than slow-growing species (Cheng et al., 2014; Kuzyakov, 2002). Yet, the effects of plant traits on rhizodeposition and RPE is still largely unknown and the link between the PES and rhizosphere processes fully remains to be explored (Cheng et al., 2014; De Deyn et al., 2008; Huo, Luo, & Cheng, 2017).

Here, we investigated how plant economic strategies affect soil carbon dynamics through rhizodeposition. Using a 'common garden' greenhouse experiment, we studied the effects of 12 grassland species selected based on a priori trait values to form a gradient of plant economic strategies and belonging to contrasting functional groups (C3 grasses, forbs and legumes). Each species was grown as monocultures for 256 days on a grassland soil under semi-natural conditions. We used a continuous ^{13}C-labelling method allowing partitioning of soil and plant sources to the ecosystem C fluxes and

pools. This enabled us to measure plant metabolic activity and root-induced change in native SOC mineralization (RPE) throughout the experiment, as well as the formation of new root-derived SOC at the end of the experiment. We hypothesized that: (H_1) plant economic strategies control SOC cycling through rhizodeposition, with fast-growing acquisitive versus slow-growing conservative species inducing fast versus slow SOC turnover in relation with enhanced rates of both SOC mineralization and formation; (H_2) legumes induce faster rhizosphere processes relative to forbs and grasses owning to their higher photosynthetic capacity (Reich et al., 2003), and higher allocation of photosynthate-C in rhizodeposition (Warembourg, Roumet, & Lafont, 2003); (H_3) grasses induce faster rhizosphere processes relative to forbs given their finer and more densely branched root systems with higher foraging ability (Roumet et al., 2016). In order to test these hypotheses and investigate the underlying mechanisms, we explored the linkages of SOC cycling processes with a large set of 15 leaf, fine-root and whole-plant traits, as well as ecosystem properties related to plant phenology, metabolic activity and primary productivity, canopy photosynthesis, rhizodeposition and soil microbial activity (Table 1).

2 | MATERIALS AND METHODS

2.1 | Species selection

We used a species pool of 12 common European grassland species, with four species included in each of three contrasting functional groups (C3 grasses, forbs and legumes). In each functional group, the species were selected along a gradient of a priori values for three economic traits, namely specific leaf area (SLA), specific root length (SRL) and relative growth rate (RGR), in order to form a gradient of plant economic strategies (Table S1 in Supporting Information). SLA is related to the light capture ability of the canopy per mass invested in leaf growth and it has a strong physiological link with leaf photosynthetic capacity. It was used as a proxy of the leaf economic spectrum (Wright et al., 2004). SRL is related to the ability of the fine-root system for foraging soil resources per mass invested in root growth. It was used as a proxy of the root economic spectrum (Roumet et al., 2016). RGR is related to plant growth potential and is well coordinated with plant economic strategies, that is, fast-growing species are more acquisitive, while slow-growing species are more conservative (Lambers & Poorter, 1992).

2.2 | Soil sampling

The soil is an SOC-rich Andosol (World Reference Base nomenclature) collected from a semi-natural grassland site in 'Laqueuille', Auvergne, France (45°38′N, 2°44′E, 1,040 m elevation). We separately sampled and sieved (4 mm) the three top mineral soil layers (0–20, 20–40 and 40–60 cm). The main soil features of the 0–20 layer are: texture, loam; pH, 5.26; SOC, 91.4 g/kg; soil C:N, 9.80; $\delta^{13}C$, −26.70 ‰ (Table S2). None of the soil layers contained carbonates.

2.3 | Experimental conditions and labelling system set-up

Bottom-capped PVC pots (diameter 10 cm, height 60 cm, with a permeable bottom-cap to allow drainage), hereafter microcosms, were filled with fresh soil of each layer according to the initial stratification and bulk density of each layer. After being stored at 4°C until further preparation, the microcosms were transferred at ambient temperature to measure the soil water-holding capacity (WHC). Each microcosm was irrigated until water saturation and weighed after 48 hr of water percolation. For each of the 12 species, three microcosms were sown to a density of seven and four plants per pot for grass and eudicot species, respectively, in order to reproduce natural density encountered in temperate grasslands (Louault, Pillar, Aufrere, Garnier, & Soussana, 2005). Four microcosms were kept unsown as unplanted control soil.

Immediately after in situ germination, the 40 microcosms were transferred in late August 2016 to a greenhouse exposed to natural light and temperature conditions (Clermont-Ferrand, temperate semi-continental climate). The experiment was performed for 256 days, until early June 2017. The greenhouse was coupled to a continuous ^{13}C-labelling system previously described by Shahzad et al. (2012) and Cros, Alvarez, Keuper, and Fontaine (2019). Briefly, ^{13}C-depleted air was produced by injecting fossil fuel-derived CO_2 ($\delta^{13}C$ = −35.23 ± 0.02 ‰, mean ± standard error) in CO_2-free air ($[CO_2]$ < 20 ppm) up to reach ambient CO_2 concentration (400 ppm). The CO_2-free air was produced using a compressor injecting ambient air into a molecular sieve (Siliporite® beads made of zeolite, 3 Å) to remove CO_2. The greenhouse was a five-side steel box buried to 60 cm depth and capped with a transparent (plexiglass screen) canopy enclosure (2.2 × 0.8 × 0.6 m). Throughout the experiment, the greenhouse was continuously supplied with re-humidified ^{13}C-depleted air during daytime. The flow was adjusted as to renew the greenhouse volume once every 2 min in order to maintain constant CO_2 concentration and $\delta^{13}C$ (Cros et al., 2019). It also allowed to maintain the temperature inside the greenhouse close to outside conditions (difference limited to 1°C in average throughout the year) by evacuating the heat generated by the greenhouse effect (Cros et al., 2019). In order to limit soil warming related to PVC exposure to sun, the top edge of the microcosms was covered with a reflective film. The microcosms were equipped with sensors of soil moisture (ECH2O EC-5, Decagon®) inserted at 5 cm and irrigation pipes connected to a programmer. Soil water content was monitored daily and drip irrigation was adjusted individually for each treatment as to maintain moisture around 85 ± 5% of WHC.

2.4 | Plant–soil microcosm CO_2 fluxes

We measured CO_2 fluxes of each microcosm on days 83, 146, 181, 209, 230 and 251 after planting, from late fall until late spring. We used the incubation method of Shahzad et al. (2012) measuring the respiration of the whole plant–soil system, corresponding to the ecosystem dark respiration. This method was chosen instead of the traditional

TABLE 1 Description of the variables studied

Abbreviation	Variable	Unit	Variation across species	
			Range	CV (%)
Soil C cycling processes				
R_{soil}	Respiration derived from native SOC mineralization	g $C\text{-}CO_2$ m^{-2} day^{-1}	0.94–5.93	43.5
RPE	Rhizosphere priming effect	%	3–295	68.5
Total RPE	Cumulative RPE for the whole experiment	%	30–117	33.6
Spring RPE	Cumulative RPE for the spring season	%	41–199	37.5
Final RPE	RPE at the end of experiment	%	26–295	70.3
qCO_2	Soil microbial metabolic quotient, that is the respiration:biomass ratio	mg $C\text{-}CO_2$ g^{-1} $SOC_{microbial}$ h^{-1}	0.63–1.01	14.9
$SOC_{microbial}$	Soil microbial carbon biomass	g C_{mic} kg^{-1} soil	0.91–1.17	7.9
R_H-SOC_{new}	Heterotrophic respiration of new root-derived SOC	mg $C\text{-}CO_2$ kg^{-1} soil day^{-1}	2.49–9.87	34.7
SOC_{new}	Stock of new root-derived SOC	g SOC kg^{-1} soil	0.12–0.98	35.0
$SOC_{balance}$	Net balance of SOC gain and loss induced by living roots, that is SOC_{new} minus Spring SOC_{primed}	g SOC m^{-2}	−66 to +22	58.4
Plant C cycling processes				
R_{plant}	Respiration derived from carbon recently fixed by plants	g $C\text{-}CO_2$ m^{-2} day^{-1}	0.49–20.49	81.7
Total R_{plant}	Cumulative R_{plant} for the whole experiment	g $C\text{-}CO_2$ m^{-2}	191–1083	43.5
Spring R_{plant}	Cumulative R_{plant} for the spring season	g $C\text{-}CO_2$ m^{-2}	125.8–891.4	44.1
Final R_{plant}	R_{plant} at the end of experiment	g $C\text{-}CO_2$ m^{-2} day^{-1}	2.3–20.4	54.1
A_{canopy}	Maximum canopy photosynthetic rate	µmol m^{-2} s^{-1}	44.0–189.8	53.3
ANPP	Aboveground net primary productivity	g plant m^{-2} day^{-1}	1.50–7.68	41.0
BNPP	Belowground net primary productivity	g plant m^{-2} day^{-1}	0.84–7.14	68.2
Fine-root NPP	Fine-root net primary productivity	g plant m^{-2} day^{-1}	0.56–4.57	61.1
Plant economic traits				
AGR	Absolute growth rate	g plant m^{-2} day^{-1}	2.33–10.53	41.0
S:R	Shoot:root ratio	g shoot g^{-1} root	0.34–3.56	54.1
SLA	Specific leaf area	mm^2/mg	8.85–38.35	34.0
LDMC	Leaf dry matter content	mg/g	132.6–341.2	31.4
LNC	Leaf nitrogen content	mg/g	7.84–37.42	48.5
A_{leaf}	Leaf light-saturated photosynthetic rate per mass	nmol g^{-1} s^{-1}	39.6–307.9	45.5
R_{leaf}	Leaf dark respiration rate per mass	nmol g^{-1} s^{-1}	4.84–17.98	36.9
RDMC	Root dry matter content	mg/g	101.6–199.9	19.9
RNC	Root nitrogen content	mg/g	4.6–19.3	53.0
R_{root}	Root dark respiration rate per mass	nmol g^{-1} s^{-1}	3.44–10.87	38.3
D_m	Mean root diameter	mm	0.12–0.45	37.1
SRL	Specific root length	m/g	52.3–534.5	76.2
RLD	Root length density	cm/cm^3	6.4–123.3	104.9
RTiD	Root tips density	$tips/cm^3$	7.0–730.6	174.3
RBI	Root branching intensity	tips/cm	0.60–6.51	75.2

CV: coefficient of variation. SOC_{primed} is the amount of native SOC mineralized by rhizosphere priming, corresponding to the difference in R_{soil} between the planted microcosm and the average of unplanted controls. RPE is the proportion of SOC_{primed} relative to the unplanted control.

method focusing exclusively on soil respiration (Cheng, 1996). This is because it is not possible to isolate the shoots from the soil with paraffin for multi-tillered grassland plant species. At each sampling, the phenological growth stage was recorded for each species according to the BBCH scale (Meier, 2003). In order to ensure similar soil moisture conditions, each microcosm was weighed and watered to 85% WHC if necessary just before measurement. Each microcosm was then sealed in an opaque, airtight PVC chamber and incubated for 24 hr in temperature-controlled conditions (21.5°C) in the laboratory. Just before the sealing, each PVC chamber was intensively ventilated for 1 min with ambient air and we took care to avoid any contamination of the chamber air by breathing. The ambient air used for the ventilation was sampled to measure the initial amount and $\delta^{13}C$ of CO_2 in the chamber at the beginning of the incubation. The constant temperature during the incubation for each sampling time allowed us to safely infer the effect of plant phenology across seasons with contrasting climatic conditions. The lack of light stopped photosynthesis, thereby preventing plant uptake of CO_2 released from the plant–soil system. Though photosynthesis did not occur during the incubation, Kuzyakov and Cheng (2001) showed that prolonged dark conditions could substantially decrease root activity and soil respiration only when the darkness exceeds 2 days. Furthermore, we are confident to capture the effect of plant photosynthetic activity on soil respiration given the time lag of about 12.5 hr between photosynthesis and soil CO_2 efflux for herbaceous plant species according to the meta-analysis by Kuzyakov and Gavrichkova (2010). Incubations always started in mid-afternoon, allowing plant photosynthesis for a large portion of the photoperiod. Previous studies using this method found a strong relationship between plant metabolic activity (R_{plant}) and native SOC mineralization (R_{soil}; Shahzad et al., 2015). At the end of incubation, the gas of each chamber was sampled and its CO_2 concentration as well as $\delta^{13}C$ were measured using a Gas Chromatograph (Clarus 480, Perkin Elmer) and an isotope laser spectrometer (CRDS Analyzer, Picarro). The amount and $\delta^{13}C$ of CO_2 derived from the plant–soil system respiration were obtained by correcting for background atmospheric CO_2 (see Appendix S1).

2.5 | Plant traits and properties

A set of 15 plant traits related to the PES were measured (Table 1, Tables S4 and S5). For leaves, it included traits related to their morphology, SLA and leaf dry matter content (LDMC); chemistry, leaf nitrogen concentration (LNC); and physiology, leaf light-saturated photosynthetic and dark respiration rate per mass (A_{leaf} and R_{leaf}). For fine-roots, it included traits related to their morphology, mean root diameter (D_m), SRL and root dry matter content (RDMC); chemistry, root nitrogen concentration (RNC); physiology, root dark respiration rate per mass (R_{root}); and architecture, root length density (RLD), root tips density (RTiD) and root branching intensity (RBI). We also included the absolute growth rate (AGR) and shoot:root ratio (S:R) as whole-plant traits.

Two days before the last plant–soil system respiration sampling in early June (day 249 after planting), we measured A_{leaf} by assessing net CO_2 assimilation using a portable infrared gas analyser connected to a 0.25 L chamber (LI-6200; LI-COR Biosciences). It was performed on three leaves and one leaf per microcosm respectively for grass and eudicot species, and the area sampled was marked for dry mass measurement at harvest. We conducted all measurements during a clear sunny day at light-saturating conditions between 14:00 and 16:00. Mean photosynthetic photon flux density (PPFD, 400–700 nm) ranged from 1,535 to 1,913 μmol m^{-2} s^{-1} and mean air temperatures ranged from 28.9 to 29.4°C.

At harvesting day following the last plant–soil system respiration sampling (day 256 after planting), three fresh leaves per microcosm were sampled, gently wiped after overnight immersion in tap water, measured for their water-saturated weight and scanned using an area meter (LI-3100C; LI-COR Biosciences). Leaves were then oven-dried (24 hr, 60°C), weighed, finely ground and analysed for LNC by dry combustion using an elemental analyser (Carlo Erba). SLA was calculated as the ratio of fresh leaf area by dry mass (DM) and LDMC as DM by fresh mass (FM).

Below-ground materials were sampled, thoroughly water-washed, sorted by material types (tap roots, rhizomes and fine roots), and fresh weighed separately for each soil layer. Trait measurements focused on fine roots, defined here as all roots excluding tap roots, sampled in the 0–20 cm soil layer. Indeed, the bulk of fine-root biomass was located in this layer (Table S3). Fine roots were sampled at five distinct locations in this soil layer, yielding a subsample of 0.650 g FM on average. The vast majority of the fine-root subsamples consisted of absorptive roots of the first three orders (Freschet & Roumet, 2017). Pioneer roots of grass species were also classified as fine roots because grasses usually have few root orders and their absorptive root pool could encompass the entire root system (Freschet & Roumet, 2017). After measuring the subsample FM, roots were stained with methylene blue (5 g/L) and rinsed in tap water. Roots were then scanned at 800 dpi with a dual lens scanner (Epson Perfection V700, Epson) to measure the mean root diameter (D_m) and total root length (L_t) using the WinRhizo Pro software (Automatic analysis, Version 2012b; Regent Instruments Inc.). All scanned roots were then oven-dried (48 hr, 60°C), weighed to determine the DM, finely ground and analysed for RNC by dry combustion using an elemental analyser. SRL was calculated as the ratio L_t:DM and RDMC as the ratio DM:FM. L_t of the soil core (L_{core}) was calculated by multiplying the total fine-root DM of the soil core by the SRL, and RLD was calculated as the ratio L_{core}:soil volume. We also sampled the entire root system of three or one randomly chosen plant individuals for grasses and eudicots, respectively, and measured the L_t and number of tips (T_i) of first three root orders using the same scanning procedure. RBI was calculated as the ratio T_i: L_t. T_i of the soil core ($T_{i\text{-}core}$) was calculated by multiplying the L_t of the soil core with RBI, and RTiD was calculated as the ratio $T_{i\text{-}core}$:soil volume.

R_{leaf} and R_{root} were measured as the CO_2 released during a 24 hr-incubation of fresh leaf and fine root materials (83 and 90 mg dry mass in average, respectively) sealed within an air-tight glass flask in the dark at 21.5°C. We acknowledge that this long incubation period

TABLE 2 Soil C cycling properties across species

Species		Total R_{soil} (RPE)	Spring R_{soil} (RPE)	Final R_{soil} (RPE)	qCO_2	$SOC_{microbial}$	R_H-SOC_{new}	SOC_{new}	$SOC_{balance}$
Grasses									
Nardus stricta (Ns)		246 ± 14b (**+30%**)	128 ± 9c (**+41%**)	1.9 ± 0.2c (+26%)	0.63 ± 0.03b	1.00 ± 0.03ab	2.5 ± 0.3c	0.12 ± 0.03b	−22 ± 13ab
Festuca rubra (Fr)		311 ± 13b (**+65%**)	173 ± 10bc (**+91%**)	2.4 ± 0.3c (+62%)	0.83 ± 0.03ab	1.03 ± 0.01ab	6.5 ± 0.5abc	0.81 ± 0.08a	+22 ± 15b
Anthoxanthum odoratum (Ao)		353 ± 18a (**+87%**)	194 ± 2b (**+115%**)	2.5 ± 0.1c (**+68%**)	0.76 ± 0.10ab	1.07 ± 0.03ab	7.2 ± 1.4abc	0.83 ± 0.08a	+4 ± 9ab
Poa trivialis (Pt)		324 ± 16ab (**+71%**)	184 ± 12bc (**+103%**)	2.1 ± 0.2c (+42%)	0.67 ± 0.02ab	1.08 ± 0.02ab	4.5 ± 0.6bc	0.60 ± 0.21ab	−16 ± 21ab
Forbs									
Chamerion angustifolium (Ca)		285 ± 4b (**+51%**)	146 ± 9c (**+62%**)	2.5 ± 0.5c (+71%)	0.64 ± 0.09b	0.98 ± 0.04b	4.4 ± 1.3bc	0.56 ± 0.09ab	+16 ± 3b
Plantago lanceolata (Pl)		373 ± 12ab (**+98%**)	215 ± 8ab (**+138%**)	2.7 ± 0.3bc (**+86%**)	0.69 ± 0.05b	1.17 ± 0.02a	6.4 ± 1.5abc	0.87 ± 0.03a	−12 ± 8ab
Rumex acetosa (Ra)		409 ± 13a (**+117%**)	208 ± 1b (**+130%**)	2.8 ± 0.2bc (**+88%**)	0.71 ± 0.09ab	0.91 ± 0.06c	3.6 ± 0.5bc	0.52 ± 0.07ab	−50 ± 8ab
Taraxacum officinale (To)		327 ± 21ab (**+73%**)	188 ± 15bc (**+108%**)	2.7 ± 0.2bc (**+82%**)	0.77 ± 0.04ab	0.97 ± 0.05bc	5.2 ± 1.3ab	0.57 ± 0.10ab	−24 ± 20ab
Legumes									
Vicia cracca (Vc)		302 ± 27b (**+60%**)	179 ± 17bc (**+98%**)	3.3 ± 0.4bc (**+122%**)	0.79 ± 0.03ab	0.95 ± 0.02bc	7.2 ± 0.7abc	0.51 ± 0.05ab	−22 ± 22ab
Lotus corniculatus (Lc)		379 ± 34a (**+101%**)	240 ± 25ab (**+166%**)	4.4 ± 0.7ab (**+201%**)	0.92 ± 0.10ab	0.92 ± 0.01c	8.4 ± 1.9ab	0.65 ± 0.12a	−66 ± 9a
Melilotus albus (Ma)		315 ± 4b (**+67%**)	186 ± 5bc (**+105%**)	3.7 ± 0.0b (**+152%**)	0.81 ± 0.06ab	0.95 ± 0.04bc	7.5 ± 0.4abc	0.64 ± 0.13a	−13 ± 21ab
Trifolium repens (Tr)		407 ± 11a (**+116%**)	270 ± 10a (**+199%**)	5.8 ± 0.4a (**+295%**)	1.01 ± 0.06a	0.91 ± 0.04c	9.9 ± 0.1a	0.98 ± 0.02a	−54 ± 12a
Unplanted control (NoPl)		189 ± 7	90 ± 5	1.5 ± 0.1	0.45 ± 0.01	0.84 ± 0.01			
Species identity	$F_{11,24}$	**7.8*****	**9.8*****	**10.1*****	**2.9***	**5.5*****	**4.2****	**5.0*****	**3.3****
Functional group (FG)	$F_{2,9}$	0.9^{ns}	1.9^{ns}	**10.8****	**5.7***	3.0†	**5.6***	0.2^{ns}	2.1^{ns}
	Contrasts			*G* = *F* < *L*	*G* = *F* < *L*	*G* > *L*	*G* = *F* < *L*		

Note: Means ± standard error are reported (n = 3 for each species, n = 4 for the unplanted control). RPEs are between brackets. Significant RPEs are in bold (t test). Different letters indicate statistically significant difference between species. Functional group abbreviations are: G, grasses; F forbs; L: legumes. For abbreviations and units of soil C cycling properties variables, see Table 1.
$^{***}p < .001$, $^{**}p < .01$, $^{*}p < .05$, $^{\dagger}p < .10$, $^{ns}P > 0.10$.

probably led to an underestimation of R_{leaf} and R_{root}, as the respiration rate could decline rapidly after excision.

After separating the remaining harvested biomass into leaf, stem and below-ground materials, including rhizomes, tap roots and fine-roots for below-ground materials, plant materials were oven-dried (48 hr, 60°C) and weighed separately. Shoot and below-ground materials were then ground and analysed separately for total C and $\delta^{13}C$ using an elemental analyzer coupled to an isotope-ratio mass spectrometer (Elementar, Langenselbold). S:R was calculated as the leaf and stem mass divided by the mass of below-ground materials. AGR was calculated by dividing the total plant living and dead biomass harvested to the number of days since planting. Above-ground, below-ground and fine-root net primary productivity (ANPP, BNPP and fine-root NPP), corresponding here to the production of above-ground, below-ground and fine-root plant biomass, were similarly calculated by dividing the mass of shoot, below-ground materials and fine-root (excluding tap roots and rhizomes) harvested to the number of days since planting. BNPP and fine-root NPP could be underestimated as the root turnover is not taken into account. To scale up photosynthesis from the leaf to the canopy level, we multiplied A_{leaf} with the microcosm leaf biomass to calculate the maximum canopy photosynthesis rate at harvest (A_{canopy}), assuming light-saturated conditions for all leaves in the canopy.

2.6 | Soil properties

At harvesting, fresh soil from the top layer (0–20 cm) was sieved (2 mm) and quickly stored at 4°C until further analyses to limit as much as possible the mineralization of rhizodeposits. After careful removing of the remaining roots, soil heterotrophic respiration (R_h) was assessed by measuring the concentration and $\delta^{13}C$ of CO_2 released during a 24 hr ex situ incubation of a 10 g fresh soil sample in airtight-sealed flasks at 21.5°C and 85% WHC. The soil microbial biomass ($SOC_{microbial}$) was measured by the chloroform–fumigation–extraction method (Vance, Brookes, & Jenkinson, 1987). A 10 g aliquot of fresh soil was extracted with 50 ml 0.5 M K_2SO_4. A second set of samples was placed in a vacuum desiccator and fumigated with chloroform for 24 hr prior to K_2SO_4 extraction as above. Extractable C was analysed using a Shimadzu 5000A TOC (Shimadzu). Microbial biomass C was calculated as the difference between the fumigated and unfumigated C extracts after conversion with a K_{ec} of 0.45 to correct for extraction efficiency (Joergensen, 1996). The microbial metabolic quotient (qCO_2) was calculated as the ratio R_h:$SOC_{microbial}$. The remaining soil was dried (48 hr, 105°C), ground and analysed for total C, N and $\delta^{13}C$ using an elemental analyzer coupled to an isotope-ratio mass spectrometer.

2.7 | Isotopic partitioning and soil C fluxes and pools calculation

The continuous labelling of plants with ^{13}C-depleted air allowed us to partition soil-derived and plant-derived CO_2 sources into the ecosystem dark respiration (Table S6). It was calculated using the following equations based on a two-source isotopic mixing model:

$$R_{soil} = R_{total} \times \frac{\delta^{13}C_{plant} - \delta^{13}C_{total}}{\delta^{13}C_{plant} - \delta^{13}C_{soil}} \quad (1)$$

$$R_{plant} = R_{total} \times \frac{\delta^{13}C_{soil} - \delta^{13}C_{total}}{\delta^{13}C_{soil} - \delta^{13}C_{plant}}, \quad (2)$$

where R_{soil} and $\delta^{13}C_{soil}$ are the CO_2 flux and $\delta^{13}C$ derived from the mineralization of native (unlabelled) SOC; R_{plant} and $\delta^{13}C_{plant}$ are the CO_2 flux and $\delta^{13}C$ derived from the mineralization of recently fixed (labelled) photosynthate-C; and R_{total} and $\delta^{13}C_{total}$ are the total CO_2 flux and $\delta^{13}C$ derived from the plant–soil system respiration. R_{plant} represents here the plant metabolic activity, including both plant autotrophic respiration and soil microbial heterotrophic respiration derived from rhizodeposits. We used the $\delta^{13}C$ of the 0–20 cm layer SOC as $\delta^{13}C_{soil}$. Indeed, the bulk of fine-root biomass was located in this layer (56% in average, Table S3), which was also richer in SOC (Table S2). Therefore, most of soil CO_2 fluxes were likely derived from the surface layer. For each specific microcosm, we used the mass-weighted $\delta^{13}C$ of its shoot and root biomass as $\delta^{13}C_{plant}$. The average $\delta^{13}C_{plant}$ was −50.01‰ (−49.34 to −51.23‰ across species, Table S3), with a range similar (around 2‰) to a previous study performed in our experimental platform with six different grassland species (Shahzad et al., 2012). This yielded an average labelling intensity of 23.31‰ relative to $\delta^{13}C_{soil}$ (−26.70‰), which is substantially larger than the labelling intensity typical yielded by the natural ^{13}C-labelling method (Cheng, 1996) as well as the traditional continuous ^{13}C-labelling method based on adding fossil fuel-derived CO_2 in a flow of ambient air (Cheng & Dijkstra, 2007), improving the accuracy of isotopic partitioning (Cros et al., 2019; Werth & Kuzyakov, 2010).

A parallel experiment running during the same period and using the same labelling system found that the isotopic composition of plant biomass was constant through time (Cros et al., 2019), indicating that the labelling remained homogeneous throughout the experiment. Further, we assumed negligible fractionation during whole-plant respiration based on Schnyder and Lattanzi (2005). The SOC $\delta^{13}C$ of the unplanted control 0–20 cm soil layer changed very few between the beginning and the end of the experience (−26.70 ± 0.02 vs. −26.62 ± 0.01‰), ensuring that the $\delta^{13}C$ of the soil-derived CO_2 remained constant throughout the experiment. Furthermore, we found similar $\delta^{13}C$ between the SOC and the CO_2 derived from the 0–20 cm soil layer of the unplanted control at the end of the experience (−26.62 ± 0.01 vs. −26.56 ± 0.10‰), ensuring that fractionation during native SOC mineralization was not an issue (Werth & Kuzyakov, 2010). However, we acknowledge that some uncertainty in $\delta^{13}C_{soil}$ remained owing to the heterogeneous $\delta^{13}C$ of the different soil layers (Table S2). A sensitivity analysis of 1‰ variation in $\delta^{13}C_{soil}$ showed nevertheless that its impact on R_{soil} and RPE estimation remained very limited (Table S7, Figure S1).

We observed that the CO_2 derived from the respiration of the unplanted microcosms was systematically depleted in ^{13}C relative to SOC (Table S6). This was most likely related to algae photosynthesis using labelled (depleted) CO_2 during daytime in the greenhouse and respiration of this labelled C back during the dark incubation (Cros et al., 2019). We thus decided to apply the same isotopic partitioning (Equations 1 and 2) on R_{total} of unplanted microcosms to get more accurate estimation of R_{soil} for the unplanted control (Table S6). We used the mean $\delta^{13}C$ of plant biomass across the 12 species as $\delta^{13}C_{algae}$ given that algae use C3 carbon fixation similarly to all our studied species (Farquhar, Ehleringer, & Hubick, 1989). We acknowledge that this partitioning relied on the assumption of similar $\delta^{13}C$ between plant and algae biomass, thus generating some uncertainty. However, we emphasize that the calculated fluxes of plant-derived respiration (R_{plant}) in the unplanted soil represented only around 10% of soil-derived respiration (R_{soil}), except for the two first sampling dates during which the CO_2 fluxes were low (Table S6). Furthermore, this would only affect the absolute quantification of the RPE, and not much the interspecific difference in RPE, as the unplanted control is the same for all the species. See Appendix S1 for further details and justification.

We calculated cumulative R_{soil} and R_{plant} by multiplying the average daily rate of CO_2 flux by the time interval between two sampling dates, and by adding the preceding CO_2 flux. Cumulative CO_2 fluxes were computed for the total experimental period, between days 83 and 251 after planting, and for the whole spring, between days 181 and 251 after planting, as we expected the fluxes to be most important during the growing season. The amount of native SOC mineralized by rhizosphere priming (SOC_{primed}) was calculated as the difference in R_{soil} between the planted microcosm and the average of unplanted controls ($R_{soil\text{-}unplanted}$). The corresponding RPE (in % relative to unplanted) was computed using the following equation:

$$RPE = \frac{SOC_{primed}}{R_{soil-unplanted}} \times 100 \quad (3)$$

Based on isotopic partitioning of CO_2 fluxes during the ex situ soil incubation, we calculated the heterotrophic respiration of new root-derived SOC (R_H-SOC_{new}) using the following equation:

$$R_H - SOC_{new} = R_H \times \frac{\delta^{13}CO_{2-soil} - \delta^{13}C_{-R_H}}{\delta^{13}CO_{2-soil} - \delta^{13}C_{root}}, \quad (4)$$

where R_H and $\delta^{13}C$-R_H are the total CO_2 flux and $\delta^{13}C$ derived from the ex situ soil incubation of the planted microcosm; $\delta^{13}CO_{2\text{-}soil}$ is the average $\delta^{13}C$ of CO_2 derived from the unplanted controls; and $\delta^{13}C_{root}$ is the root biomass $\delta^{13}C$ of the planted microcosm. As R_H-SOC_{new} is ultimately derived from the mineralization of C compounds recently fixed by plants and transferred to the soil, we used it as a proxy of microbial utilization of rhizodeposits at harvesting.

We also calculated the formation of new root-derived SOC (SOC_{new}) derived from rhizodeposition and root turnover at the end of the experiment using the following equation:

$$SOC_{new} = SOC_{total} \times \frac{\delta^{13}SOC_{soil} - \delta^{13}SOC_{total}}{\delta^{13}SOC_{soil} - \delta^{13}C_{root}}, \quad (5)$$

where SOC_{total} and $\delta^{13}SOC_{total}$ are the SOC concentration and $\delta^{13}C$ of the planted microcosm; $\delta^{13}SOC_{soil}$ is the average $\delta^{13}C$ of SOC from the unplanted controls; and $\delta^{13}C_{root}$ is the root biomass $\delta^{13}C$ of the planted microcosm. Senesced above-ground plant material lying on the soil surface was regularly collected, ensuring that new SOC was root-derived.

Assuming that most of both native SOC mineralization and SOC formation occurred in the 0–20 cm soil layer during spring (owing that most of R_{plant} fluxes occurred during this early growing season), we calculated the balance between the amount of SOC gained by formation of new root-derived SOC versus lost by rhizosphere priming using the following equation:

$$SOC_{balance} = SOC_{new} - Spring\ SOC_{primed}. \quad (6)$$

2.8 | Statistical analyses

Since our aim was to focus on interspecific differences, microcosm was used as statistical unit for testing species identity effect (n = 3 microsms per species) but species mean was used as statistical unit in all others analyses unless specified (n = 12 species). We first tested the effects of species identity (Sp) and functional groups (FG) on soil and plant C cycling processes using one-way ANOVAs with either Sp or FG as fixed factor. Post-hoc comparisons were performed using Tukey's HSD tests.

For the analysis of plant–soil system CO_2 flux time series, we further incorporated the factor 'days after planting' (DAP) and we adopted a linear mixed-effects modelling approach by including individual microcosm as a random effect to deal with the repeated measures design (*lme* function in the *nlme* package). A correlation structure term (*corAR1* function) was included to take into account temporal autocorrelation of each microcosm. To assess how RPE temporal dynamics was driven by plant phenological development (phenology) and metabolic activity (R_{plant}), we performed regression by either phenology or R_{plant}, with FG and interactions as covariates.

In order to investigate the linkages between soil C dynamics and plant economic strategies, we performed ordination of soil C cycling properties constrained by the 15 plant traits using a redundancy analysis (function *rda* in the *vegan* package). Plant C cycling properties were fitted in the ordination space as passive variables (function *envfit* in the *vegan* package). The significance of the overall constrained ordination as well as of each axis were tested using permutation tests (function ANOVA in the *vegan* package). Microcosm was used as statistical unit, but the permutation tests were restricted at the between species level (1,000 permutations, function *how* in the *permute* package).

Each soil C cycling variable was also related to plant traits by multimodel inference. In order to avoid comparing too many candidate models (Burnham & Anderson, 2002), we first reduced the 15 plant traits to five components of plant functioning based on their correlation structure (Table S5): (a) plant growth, including AGR; (b)

plant biomass allocation, including S:R; (c) leaf economics spectrum (LES), including SLA, LDMC, LNC, A_{leaf} and R_{leaf}; (d) root economics spectrum (RES), including RDMC, RNC, and R_{root}; (e) soil exploration spectrum (SES), including Dm, SRL, RLD, RTiD and RBI. LES, RES and SES were each reduced to a single variable by performing principal component analyses and using the first axis scores (Figure S2). Selection of multiple regression models was performed based on Akaike Information Criterion (AICc, function *dredge* in the package *MuMIn*) to establish a confidence set of up to five models with ΔAICc < 2 from all possible combination of the five traits components. The relative importance of the factors was then calculated as the sum of Akaike weights (w_i) derived for all the models in which the factor occurred, and we used a model averaging approach to compute w_i-weighted average effect sizes (β_{st}, range-standardized regression coefficients). Finally, relationships between key soil and plant C cycling properties were explored by simple regressions.

All analyses were performed using R v3.4.3 (R Core Team, 2017). The normal distribution and homogeneity of variances of the model residuals were checked and data were log-transformed when necessary.

3 | RESULTS

3.1 | Temporal dynamics and drivers of the RPE

All species induced a positive RPE, corresponding to an acceleration of native SOC mineralization (R_{soil}) relative to the unplanted control for the whole-experiment (Figure 1a, Table 2). The RPE increased over time during the growing season in spring to reach its highest level around the flowering stage (Figure 1a,b,c, Table S8).

There were large differences among species in RPE and plant metabolic activity (R_{plant}), which were both higher for *Trifolium repens* and *Lotus corniculatus*, and lower for *Nardus stricta* and *Chamerion angustifolium* (Table 2, Figure 1a, Tables S8 and S9). RPE and R_{plant} were also higher for legume species at the end of the experience.

We observed that the increase in RPE was mediated by the temporal dynamics of phenology and R_{plant}. The phenological development of fast-growing species was quicker (Figure S3), and was linked with large levels of R_{plant} and RPE earlier in the growing season (Figure 1c and Figure S3). The increase in R_{plant} and RPE with phenological development was stronger for legume species. In turn, the increase in R_{plant} was associated to an increase in RPE, which was stronger for legumes (Figure 1d).

3.2 | Soil C cycling and plant economic strategies linkages

The redundancy analysis demonstrated that the plant economic traits were tightly related to soil C cycling properties ($F_{15,20}$ = 4.4, p > .001), explaining 76.6% of variation (Figure 2). The first axis (RDA1) explained a large portion of variation (47.2%, $F_{1,28}$ = 54.4, p < .001), whereas the second axis explained only 14.1% ($F_{1,28}$ = 16.3, p = .245). RDA1 was positively related to final, spring and total RPE, R_H-SOC_{new}, qCO_2 and SOC_{new}, and negatively to $SOC_{balance}$ and $SOC_{microbial}$ (Table S10). The plant economic traits AGR, S:R, A_{leaf}, LNC, SLA, R_{root} and RNC were positively related to RDA1, while LDMC and RDMC were negatively related. This first axis was interpreted as a 'plant economics spectrum', with the acquisitive versus conservative strategies associated with high versus low leaf photosynthetic capacity (LES), root metabolic activity (RES) and allocation of biomass above-ground, and fast versus slow growth rates on the negative versus positive sides. The root traits SRL, RTiD, RBI and RLD related to soil exploration (SES), commonly associated with the acquisitive strategy, were however negatively related to RDA1, and conversely for the D_m. Plant properties such as final, spring and total R_{plant}, A_{canopy} and ANPP were positively related to RDA1. Legumes species had higher RDA1 scores.

Among economic traits, the best predictors of RPE were predominantly whole-plant and leaf traits. Final and spring RPE were related positively to AGR, S:R, and LES (Table 3, Figure S4), and total RPE was related positively with AGR and LES (Table S10). R_H-SOC_{new} and qCO_2 were higher for legumes species (Table 2). R_H-SOC_{new} was related positively to AGR, S:R, and RES (Table 3). qCO_2 was positively related to AGR, S:R, LES and RES (Table S11). $SOC_{microbial}$ tended to be lower for legume relative to grass species (Table 2), and was related negatively to LES (Table S11). SOC_{new} was related positively to AGR and to a lower extent S:R, but was less well-explained by economic traits compared to RPE (Tables 3 and Table S11). $SOC_{balance}$ was related negatively to AGR and LES (Table S11).

Exploring interspecific relationships between key soil and plant C cycling properties, we found strong positive linkage between A_{canopy} and final RPE (Figure 3a, r^2 = .74). A_{canopy} was also positively related to both R_H-SOC_{new} and qCO_2 (Figure S5a,b), and was higher for legume relative to grass species (Table S9). In turn, R_H-SOC_{new} was positively associated with final RPE (Figure 3b, r^2 = .72) and qCO_2 (Figure S5c). Finally, qCO_2 was itself positively related to final RPE (Figure 3c, r^2 = .79). Final R_{plant} was also an excellent predictor of final RPE, with a positive relationship (Figure S5d; r^2 = .85).

Spring and total RPE were both positively related to ANPP (Figure 3d, Figure S5e), but not with fine-root NPP (Figure S5f,g). SOC_{new} was positively related to ANPP (Figure 3e), and tended to be also positively related to fine-root NPP (Figure S5h).

The amounts of SOC gains and losses induced by living roots were positively related to each other (Figure S5i), with an overall weak net SOC loss across species (Figure 3f). However, several species deviated from this pattern: *T. repens* and *L. corniculatis* induced a large net SOC loss, while *Festuca rubra* and *C. angustifolium* conversely induced a moderate net SOC gain. Indeed, $SOC_{balance}$ was negatively related to A_{canopy} (Figure 3f).

4 | DISCUSSION

The primary aim of this study was to investigate how plant economic strategies affect soil carbon cycling processes related to

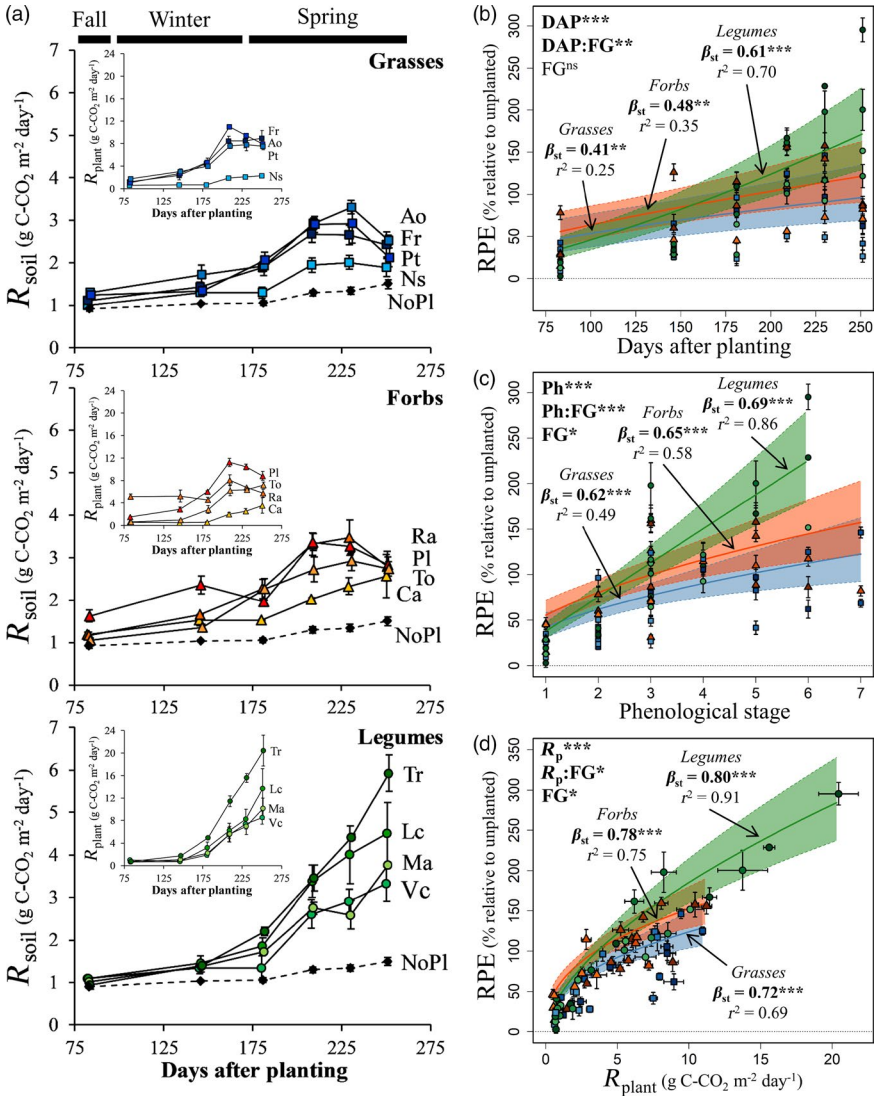

FIGURE 1 Temporal dynamics and drivers of the rhizosphere priming effect (RPE): (a) Soil-derived respiration (R_{soil}) for each species over the 256 days of the experiment. The relative difference in R_{soil} between the planted treatments and the unplanted control represents the RPE. The inset shows plant-derived respiration (R_{plant}). (b–d) Relations of the RPE with the time after planting (DAP), the phenological development (Ph), and the plant metabolic activity (R_{plant}). Functional groups (FG) are represented by blue squares, orange triangles and green circles for grasses, forbs and legumes species, respectively. Absolute growth rates are represented by lighter to darker colours from slow-growing to fast-growing species, respectively. Black diamonds and dashed lines represent the unplanted control (NoPl). The means of each treatment are plotted, and error bars represent ± standard error (n = 3 for each species, n = 4 for the unplanted control). For b–d, statistical significance of each factor effect is reported in the upper part. Regressions have been performed using species mean as statistical unit (n = 12 species for six sampling times). Slope (β_{st}, range-standardized regression coefficient), statistical significance, coefficient of determination (marginal r^2, variation explained by fixed factors) and 95% confidence interval (grey band) of each separate regression are also reported. The BBCH scale of phenological development includes the following stages: 0, germination, sprouting or bud development; 1, leaf development; 2, formation of side shoots, tillering; 3, stem elongation or rosette growth; 4, development of vegetatively propagated organs; 5, main shoot inflorescence emergence, heading; 6, flowering; 7, development of fruit; 8, ripening or maturity of fruit and seed; 9, senescence. For abbreviations of species names, see Table 2. ***p < .001, **p < .01, *p < .05, ^{ns}p > .10 [Colour figure can be viewed at wileyonlinelibrary.com]

native SOC mineralization and formation through rhizodeposition and associated rhizosphere processes. In contrast with previous studies typically including up to four species only (Cheng et al., 2014; Wang et al., 2016; Yin et al., 2018), we used here a relatively large pool of 12 grassland species featuring contrasting economic traits (Tables 1 and 2). For instance, absolute growth rate (AGR) varied five-fold (2.3–10.5 g plant m^{-2} day^{-1}), leaf photosynthetic rate (A_{leaf}) varied eight-fold (39.6–307.9 nmol g^{-1} s^{-1}) and root length density (RLD) varied nineteen-fold (6.4–123.3 cm/cm^3) among species. Our species pool was spread along a trait syndrome corresponding to the PES (Figure 2). The acquisitive versus conservative strategies were associated with a fast versus slow growth (AGR) as well as a high versus low allocation of biomass above-ground (S:R), leaf photosynthetic capacity (A_{leaf}) and root metabolic activity (R_{root}; Freschet, Cornelissen, Logtestijn, & Aerts, 2010; Kramer-Walter

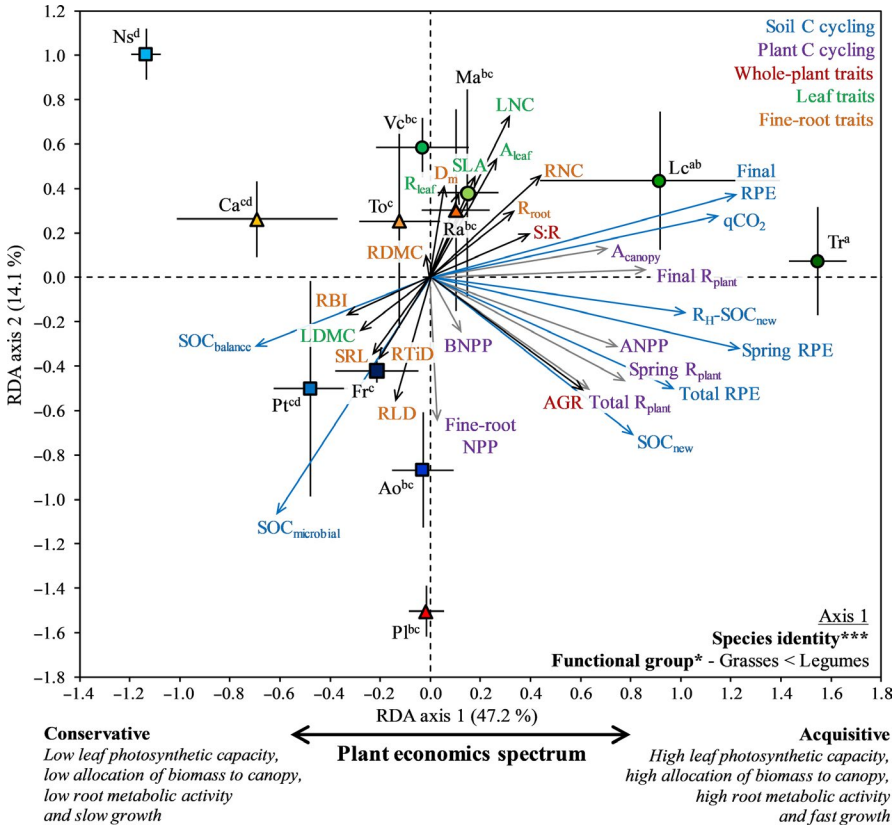

FIGURE 2 Ordination of soil C cycling properties (blue arrows) constrained by plant traits (dark arrows) using a redundancy analysis. Plant C cycling properties (grey arrows) are fitted in the ordination space as passive variables. The means of species coordinates are plotted in the ordination space. Error bars represent ± standard error (n = 3). Functional groups are represented by blue squares, orange triangles and green circles for grasses, forbs and legumes species, respectively. Plant growth rates are represented by lighter to darker colours from slow-growing to fast-growing species, respectively. The constrained ordination was significant for axis 1, but not for axis 2 (Table S9). Statistical significance of the effects of species identity and functional group on axis 1 scores is reported in bottom right. Species with different letters have statistically significant difference in their coordinates on axis 1. For abbreviations of species names and variables, see Tables 1 and 2. ***p < .001, *p < .05 [Colour figure can be viewed at wileyonlinelibrary.com]

et al., 2016; Reich, 2014). Acquisitive species were here surprisingly associated with a thicker and less densely branched root system (D_m, SRL, RTiD and RBI), in contrast with previous studies demonstrating the existence of a single root economics spectrum (Prieto et al., 2015; Roumet et al., 2016). However, an increasing number of studies highlighted that fine-root traits are multidimensional, with fine-root morphological and architectural traits related to water and nutrient foraging being not necessarily well coordinated with the PES (Kramer-Walter et al., 2016; Ma et al., 2018; Weemstra et al., 2016).

All species enhanced the rate of native SOC mineralization, but this RPE substantially differed across species (Table 1). It varied eleven-fold by the end of the experiment, with a range from +26% for *Nardus stricta* to +295% for *Trifolium repens* (Table 2). Similarly, the formation of new root-derived SOC (SOC_{new}) varied nine-fold, with a range from 0.10 for *N. stricta* to 0.91 g SOC/kg soil for *T. repens*. Here, we demonstrated that plant economic traits and associated strategies are strong drivers of this interspecific variation in SOC cycling processes (Figure 2).

4.1 | Effects of plant economic strategies on soil carbon mineralization and rhizosphere priming

The absolute growth rate (AGR) was one of the best predictors of the RPE among plant economic traits (Table 3). This shows that inherent variation in growth rate among plants control the rate of native SOC mineralization, with high RPE for fast-growing species associated with high primary productivity. We further observed that the temporal dynamics of RPE was affected by plant growth (Figure 1). Specifically, the increase in RPE during the growing season was stronger for fast-growing species in relation with their faster phenological development and associated increase in plant metabolic activity. This shows that phenology can modulate plant species effects on RPE, as previously observed for crop species (Cheng et al., 2003).

The RPE was also strongly linked to biomass allocation patterns and leaf photosynthetic capacity, in close coordination with inherent growth rate (Lambers & Poorter, 1992). Fast-growing species are generally associated with larger allocation of biomass above-ground (Poorter et al., 2012). This led here to higher RPE as highlighted by its positive relationship with the shoot:root ratio (S:R, Table 3). This is consistent with the strong positive relationship observed between above-ground net primary productivity (ANPP) and RPE (Figure 3d), in agreement with a recent meta-analysis (Huo et al., 2017). Similarly, fast-growing species are globally associated with high leaf photosynthetic rate per mass (A_{leaf}), in relation with high leaf specific area (SLA) and nitrogen content (LNC) and low dry matter content (LDMC; Reich et al., 2003). We found here a striking positive linkage between the leaf economic spectrum (LES, Wright et al., 2004) primarily related to A_{leaf} and the rhizosphere priming (Table 3). Accordingly, we observed a strong positive relationship between the canopy photosynthetic rate (A_{canopy}) and RPE (Figure 3a). Previous studies suggesting a linkage between A_{canopy} and soil C cycling used only indirect methods

TABLE 3 Results of the selection procedure of multiple regression models relating final and spring RPE, R_H-SOC_{new} and SOC_{new} to plant economic traits (n = 12 species)

Plant economic traits					Model goodness-of-fit		
AGR	**S:R**	**LES**	**RES**	**SES**	**ΔAICc**	w_i	r^2
Final RPE							
0.63***	**0.48*****	**0.65*****			0.00	1.00	.95
0.63	0.48	0.65			Overall β_{st}		
1.00	1.00	1.00			Sum of w_i		
Spring RPE					ΔAICc	w_i	r^2
0.79***	**0.34****	**0.44****			0.00	1.00	.93
0.79	0.34	0.44			Overall β_{st}		
1.00	1.00	1.00			Sum of w_i		
R_H-SOC_{new}					ΔAICc	w_i	r^2
0.51**	**0.47***		**0.50****		0.00	1.00	.82
0.51	0.47		0.50		Overall β_{st}		
1.00	1.00		1.00		Sum of w_i		
SOC_{new}					ΔAICc	w_i	r^2
0.50*					0.00	0.64	.45
0.57**	0.33†				1.11	0.36	.60
0.53	0.33				Overall β_{st}		
1.00	0.36				Sum of w_i		

Note: The range-standardized regression coefficients (β_{st} – effect size) and statistical significance of each predictor are reported. Weighted average β_{st} is the predictor mean β_{st} based on model averaging approach using Akaike weights (w_i). Models with ΔAICc < 2 and variance inflation factor (VIF) < 4 were included in the confidence models set. LES, RES and SES are the principal component analysis first axis scores of trait subsets related to the leaf economics spectrum, root economics spectrum and soil exploration spectrum, respectively (Figure S2). LES explained 64.6% of variance and is related positively to A_{leaf}, SLA, LNC, and R_{leaf}, and negatively to LDMC; RES explained 58.7% of variance and is related positively to R_{leaf} and RNC, and negatively to RDMC; SES explained 82.0% of variance and is related positively to SRL, RLD, RTiD, and RBI, and negatively to D_m (Table S5). For abbreviations of soil C cycling properties and plant traits, see Table 1.
$^{***}p$ < .001, $^{**}p$ < .01, $^{*}p$ < .05 $^{\dagger}p$ < .10.

such as clipping and shading (Bahn, Schmitt, Siegwolf, Richter, & Brüggemann, 2009; Craine, Wedin, & Chapin, 1999; Kuzyakov & Cheng, 2001; Shahzad et al., 2012). Here, we provide direct evidence that plant photosynthetic activity controls native SOC mineralization, and is a major driver of interspecific variation in rhizosphere priming. This finding contributes to the emerging view that recent photosynthesis should be taken into account to better understand soil carbon dynamics (Högberg & Read, 2006).

We also found that the heterotrophic respiration of new root-derived SOC (R_H-SOC_{new}, a proxy of microbial utilization of rhizodeposits) was positively related to both A_{canopy} and RPE (Figure 3b). This suggests that plant photosynthesis control on rhizosphere priming is ultimately driven by the supply of root exudates such as organic acids destabilizing mineral-organic associations (Keiluweit et al., 2015) and labile carbohydrates providing energy and stimulating microbial activity and exoenzyme production, in support of the 'microbial activation hypothesis' (Cheng & Kuzyakov, 2005; Kuzyakov, 2002). R_H-SOC_{new} was positively related to AGR and S.R (Table 3), showing that fast-growing acquisitive species with high ANPP invest more photosynthate-C in rhizodeposition (Guyonnet, Cantarel, Simon, & Haichar, 2018). R_H-SOC_{new} was also interestingly related positively to the RES primarily related to root dark respiration rate per mass (R_{root}, Table 3), suggesting that high root metabolic activity was associated with enhanced rhizodeposition supply. The large R_H-SOC_{new} of legumes species (Figure 2 and Table 2), in line with a previous study (Warembourg et al., 2003), could also be linked to the formation of N-fixing symbiotic associations, which represent a high energetic cost and require a large allocation of C-photosynthate below-ground (Vitousek & Howarth, 1991). Furthermore, we found that the microbial metabolic quotient (qCO_2) was positively related to both R_H-SOC_{new} and RPE (Figure 3c). This suggests that an enhanced rhizodeposition by acquisitive species increase microbial allocation of energy to mineralization activities relative to growth (Shahzad et al., 2015), potentially in relation with a reduction in N availability by enhanced root N uptake, a lower carbon use efficiency and a faster turnover of microbial biomass (Chen et al., 2018; Sinsabaugh, Moorhead, Xu, & Litvak, 2017). This variation in microbial activity could also potentially be linked to the selection of rhizosphere microbiomes with contrasting SOC mineralization abilities by plant species with different economic strategies (Pascault et al., 2013; Schimel & Schaeffer, 2012).

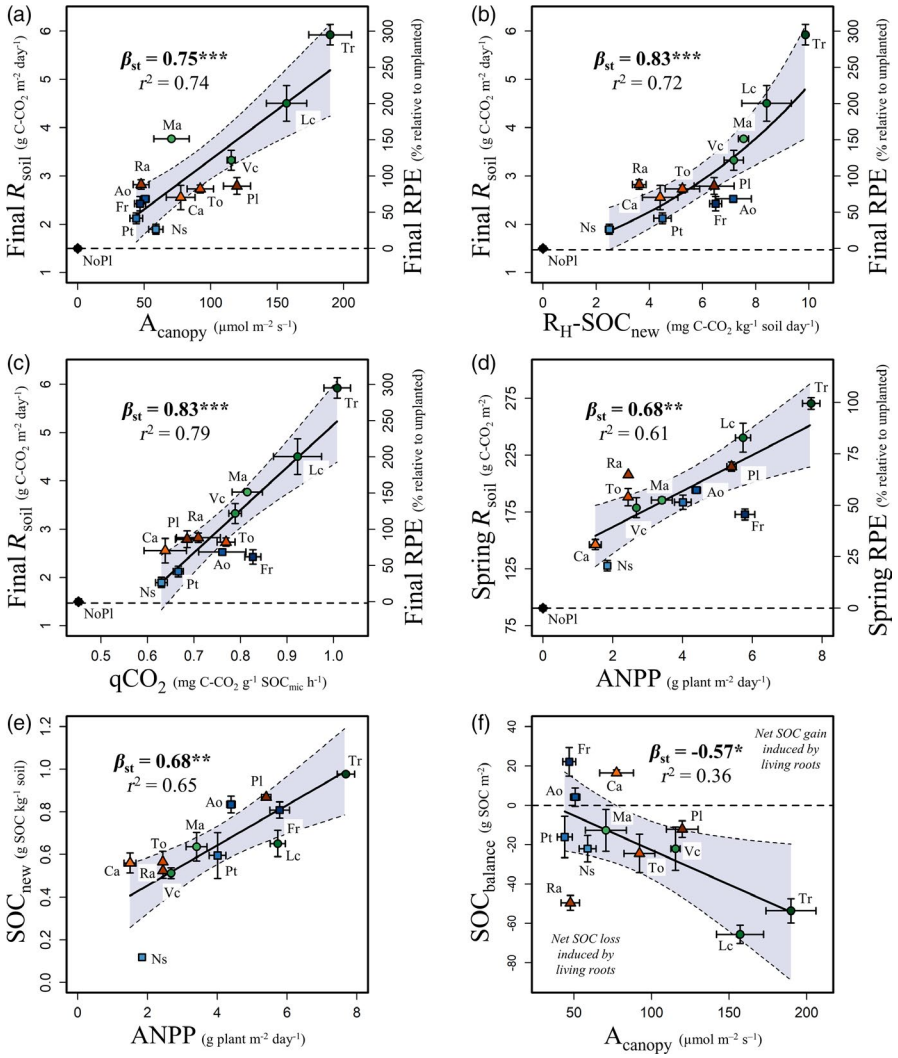

FIGURE 3 Drivers of soil carbon cycling processes: (a–c) Relation of the respiration derived from native SOC mineralization (Final R_{soil}) and associated rhizosphere priming effect (Final RPE) with the canopy photosynthetic rate (A_{canopy}), the heterotrophic respiration of new root-derived SOC (R_H-SOC$_{new}$) and the microbial metabolic quotient (qCO$_2$) measured at the end of the experiment. (d–e) Relation of the spring cumulative R_{soil} and associated RPE as well as with the new root-derived SOC (SOC$_{new}$) with the above-ground net primary productivity (ANPP). (f) Relation of the SOC$_{balance}$ (gain minus loss of SOC induced by living roots) with A_{canopy}. Functional groups (FG) are represented by blue squares, orange triangles and green circles for grasses, forbs and legumes species, respectively. Absolute growth rates are represented by lighter to darker colours from slow-growing to fast-growing species, respectively. Black diamonds and dashed lines represent the unplanted control (NoPl). The means of each treatment are plotted, and error bars represent ± standard error (n = 3 for each species, n = 4 for the unplanted control). Regressions have been performed using species mean as statistical unit (n = 12 species). Slope (β_{st}, range-standardized regression coefficient), statistical significance, coefficient of determination (r^2) and 95% confidence interval (grey band) of each regression are reported. Significance: *, **, and *** indicates p < .05, p < .01, and p < .001 [Colour figure can be viewed at wileyonlinelibrary.com]

Altogether, our results revealed in accordance with our hypotheses H_1 and H_2 that plant species effects on rhizosphere priming are tightly coupled to their economic strategies of light and CO_2 resource acquisition and processing, integrated at the whole-plant scale (Lambers & Poorter, 1992; Reich, 2014; Wright et al., 2004). Plant species with an acquisitive strategy induced large RPE, in association with a high inherent growth rate, high investment in light interception and CO_2 assimilation capacities, and low investment in tissue longevity (Figure 2). The large RPE of acquisitive species was indeed related to their high canopy photosynthesis activity coupled to high leaf photosynthetic capacity and large net primary productivity allocated above-ground, as well as high root metabolic activity, rhizodeposition and soil microbial activity. The higher RPE of legumes species can be largely explained by their acquisitive strategy, in accordance with hypothesis H_2.

The high RPE of acquisitive plants might also be related to their potentially high rhizodeposition rate of N-rich compounds, such as amino acids, resulting in a low C:N stoichiometric ratio of their rhizodeposits and providing enough N resource for microbial growth and exoenzyme synthesis (Carrillo et al., 2017; Chen et al., 2014; Drake et al., 2013). The effect of plant species identity and economic traits on N rhizodeposition and C:N rhizodeposition stoichiometry remained

however largely unknown (Jones et al., 2009). Furthermore, the supply of exudates with lower C:N ratio has been found to increase the biomass but not the respiration of soil microbes (Drake et al., 2013), while we conversely observed here that acquisitive species were associated with higher microbial activity relative to their biomass (qCO_2, Figures 2 and 3c).

Fine-root growth was unrelated to the RPE (fine-root NPP, Figure 2), in line with a recent meta-analysis (Huo et al., 2017). Furthermore, fine-root morphological and architectural traits related to soil exploration were poor predictors of the RPE (Figure 2, Table 3), in accordance with previous studies (Carrillo et al., 2017; Wang et al., 2016). This gives weak support for the hypothesis (H_3) that acquisitive species featuring fine and densely branched root systems with high foraging ability induce larger RPE (De Deyn et al., 2008; Kuzyakov, 2002; Personeni & Loiseau, 2004). Plant economic traits related to C-photosynthate production (A_{canopy}) and supply to the soil through rhizodeposition (R_H-SOC_{new}) seems to be more important determinants of the RPE than fine-root morphological and architectural traits shaping the volume of rhizospheric soil and spatial distribution of rhizodeposition. This result should however be taken with cautious as fine-root trait values are known to sometimes differ between plants growing in pots or in the field (Freschet et al., 2017). Species with thick roots and low SRL are usually associated with high level of mycorrhizal colonization (Ma et al., 2018). This might allow an efficient distribution of rhizodeposits to the soil through the mycorrhizosphere (Johnson, Leake, Ostle, Ineson, & Read, 2002; Jones et al., 2004), compensating for their low root length relative to growth investment.

4.2 | Effects of plant economic strategies on soil carbon formation and turnover

The formation of new root-derived SOC (SOC_{new}) was positively related to AGR and S:R (Table 3), with higher SOC_{new} for fast-growing species with high above-ground net primary productivity (Figure 3e). This confirms that plants can promote the formation of SOC by the supply of rhizodeposits (Dijkstra & Cheng, 2007; Sokol et al., 2018). These labile plant inputs, mostly exudates but also fine root litter, with typically fast turnover could enhance the production of microbial residues stabilized in mineral-organic associations as well as soil aggregates occluding organic matter (Cotrufo et al., 2013; Kallenbach, Frey, & Grandy, 2016; Liang, Schimel, & Jastrow, 2017; Rasse, Rumpel, & Dignac, 2005). However, we found that SOC_{new} formation was less well related to economic traits than RPE (Table 3). Furthermore, acquisitive traits were here surprisingly associated to a reduction of microbial biomass (Figure 2), which is considered as a major source of SOC formation (Miltner, Bombach, Schmidt-Brücken, & Kästner, 2012). Soil microbes were perhaps constrained by low N availability due to higher root N uptake, which might induce a shift in the allocation of microbial energy to mineralization activities at the expense of growth (Chen et al., 2018; Drake et al., 2013; Shahzad et al., 2015), thus ultimately impeding the formation of SOC_{new} (Bradford, Keiser, Davies, Mersmann, & Strickland, 2013). The stabilized SOC could also be destabilized by enhanced rhizosphere priming, thus perhaps compromising the larger SOC formation by acquisitive species over the long-term. Several studies have shown that higher rhizodeposition associated with CO_2 enrichment can lead to an accelerated turnover of new root-derived SOC and a decline in long-term SOC formation (Heath et al., 2005; Phillips et al., 2012; van Groenigen et al., 2017).

Taken together, our results support our hypothesis H_1 that fast-growing acquisitive versus slow-growing conservative species lead to a fast versus slow turnover of SOC through rhizodeposition (Figure 2). Importantly, this finding demonstrates that the linkage between plant economic strategies and ecosystem processes previously found for primary production and litter decomposition can be extended to carbon cycling in the mineral soil (Reich, 2014). Furthermore, it shows that the control of plant economic strategies on soil biogeochemistry can be more important than previously thought since it does not only affect the decomposition of its own litter, but also that of the large reserve of SOC in its rhizosphere.

We interestingly observed a substantial decoupling of the relationship between the formation and mineralization of SOC according to plant economic strategies. Acquisitive species associated with high photosynthetic activity and rhizodeposition promoted disproportionately large loss of native SOC relative to the formation of new root-derived SOC. Though it should be considered with great caution given the uncertainty in our estimation of both SOC loss and gain, our results suggest that it led to a net SOC loss (Figure 3f), at least during the growing period. This destruction of soil organic matter could ultimately promote the availability of mineral nutrients for plants (Dijkstra, Bader, Johnson, & Cheng, 2009), allowing the rapid growth of these species. This pattern might be different in fall, during which plant senescence occur and SOC formation could be favored by the pulse of litter input and the decline in plant rhizodeposition and N uptake (Fontaine et al., 2011; Kuzyakov, 2002). Further research involving longer-term experiments spanning contrasting seasons are necessary to better understand the effects of plant economic strategies on SOC storage through rhizodeposition as well as litter supply. Field-based studies would be also necessary to confirm that our findings based here on a microcosm experiment can be extrapolated to natural ecosystems, though continuous ^{13}C-labelling under field conditions remains methodologically very challenging.

4.3 | Implications for plant species control over long-term soil C sequestration

A theoretical framework has been proposed which states that fertile ecosystems dominated by fast-growing acquisitive species would support fast decomposition resulting in low net accumulation of SOC, whereas infertile ecosystems dominated by slow-growing conservative species would be associated with slow decomposition

promoting high SOC sequestration (Wardle et al., 2004). Indeed, a large number of studies provides empirical evidence that temperate grasslands dominated by acquisitive species are associated with lower SOC storage than these dominated by conservative species (Garnier et al., 2004; Grigulis et al., 2013; Klumpp, Soussana, & Falcimagne, 2007). The most common interpretation is that it results from the production of high-quality litter that decomposes fast and leads to a low accumulation of SOC (Fortunel et al., 2009; Quested, Eriksson, Fortunel, & Garnier, 2007). However, the view that litter quality determines long-term decomposition rates in the mineral soil and that long-term SOC sequestration is ultimately driven by the selective preservation of recalcitrance compounds has been challenged (Schmidt et al., 2011). There is even growing evidence supporting the hypothesis that labile plant constituents lead to larger SOC formation by promoting more efficient production of microbial compounds, which are thought to be the main precursors of stable SOC (Cotrufo et al., 2013, 2015; Liang et al., 2017).

Our results suggest that an alternative but not necessarily mutually exclusive mechanism could be at play. Indeed, the low SOC storage of temperate grasslands dominated by acquisitive species could be explained by the large loss of native SOC induced by rhizosphere priming relative to its gain by the formation of new root-derived SOC, ultimately leading to a net SOC loss (Figure 3f). This alternative interpretation is consistent with a previous study demonstrating that living root activity of fast-growing acquisitive plants adapted to intense grazing triggers SOC loss by enhancing soil microbial activity and particulate organic matter decomposition (Klumpp et al., 2009). Here, we extended this finding to the total SOC, which could also involve the priming of more stabilized SOC pools (Dijkstra & Cheng, 2007; Fontaine et al., 2007).

In conclusion, our study demonstrates that rhizodeposition is a major mechanism through which plant economic strategies of grassland species control soil carbon dynamics. Acquisitive versus conservative species were associated to high versus low rates of photosynthesis and rhizodeposition, in turn leading to fast versus slow SOC turnover. These novel insights point to the importance of incorporating plant economic traits and rhizosphere processes in Earth system models to provide more realistic projections of soil carbon dynamics (Finzi et al., 2015; Luo et al., 2016; Perveen et al., 2014; Reich, 2014). Given the important shifts in vegetation composition to be expected worldwide with global change (Nolan et al., 2018), this would be critical to improve our predictions of terrestrial ecosystem C dynamics and climate feedbacks (Heimann & Reichstein, 2008).

ACKNOWLEDGEMENTS

This study was financially supported by the ANR project DEDYCAS (ANR 14-CE01-0004) led by J. Balesdent. We thank the certified facility in Functional Ecology (PTEF OC 081) from UMR 1137 EEF and UR 1138 BEF in the research centre INRA Nancy-Lorraine for its contribution to isotopic analysis of plant and soil samples. The PTEF facility is supported by the French National Research Agency through the Laboratory of Excellence ARBRE (ANR-11-LABX-0002-01). We greatly thank S. Revaillot, L. Andanson, A. Salcedo, K. Klump, O. Darsonville, H. Desmyttère and C. Hossann for their technical support, J. Pottiez, J. Bloor and C. Roumet for their advice, as well as C. Spitzer, D.A. Wardle, G. Freshet and two anonymous reviewers for their valuable comments and corrections.

AUTHORS' CONTRIBUTIONS

L.H. and S.F. conceived the ideas and designed methodology; L.H., C.C., C.P.-C., V.R. and S.F. collected the data; L.H. analysed the data and led the writing of the manuscript. All authors contributed critically to the drafts and gave final approval for publication.

DATA AVAILABILITY STATEMENT

Data available from the Dryad Digital Repository: https://doi.org/10.5061/dryad.040jp22 (Henneron et al. 2019)

ORCID

Ludovic Henneron https://orcid.org/0000-0002-3979-0543

REFERENCES

Bahn, M., Schmitt, M., Siegwolf, R., Richter, A., & Brüggemann, N. (2009). Does photosynthesis affect grassland soil-respired CO_2 and its carbon isotope composition on a diurnal timescale? *New Phytologist*, *182*, 451–460.

Bardgett, R. D., Bowman, W. D., Kaufmann, R., & Schmidt, S. K. (2005). A temporal approach to linking aboveground and belowground ecology. *Trends in Ecology & Evolution*, *20*, 634–641. https://doi.org/10.1016/j.tree.2005.08.005

Bardgett, R. D., Mommer, L., & De Vries, F. T. (2014). Going underground: Root traits as drivers of ecosystem processes. *Trends in Ecology & Evolution*, *29*, 692–699. https://doi.org/10.1016/j.tree.2014.10.006

Bradford, M. A., Keiser, A. D., Davies, C. A., Mersmann, C. A., & Strickland, M. S. (2013). Empirical evidence that soil carbon formation from plant inputs is positively related to microbial growth. *Biogeochemistry*, *113*, 271–281. https://doi.org/10.1007/s10533-012-9822-0

Burnham, K. P., & Anderson, D. R. (2002). *Model selection and multimodel inference: A practical information-theoretic approach*. New York, NY: Springer Science & Business Media.

Carrillo, Y., Bell, C., Koyama, A., Canarini, A., Boot, C. M., Wallenstein, M., & Pendall, E. (2017). Plant traits, stoichiometry and microbes as drivers of decomposition in the rhizosphere in a temperate grassland. *Journal of Ecology*, *105*, 1750–1765. https://doi.org/10.1111/1365-2745.12772

Chen, L., Liu, L., Mao, C., Qin, S., Wang, J., Liu, F., … Yang, Y. (2018). Nitrogen availability regulates topsoil carbon dynamics after permafrost thaw by altering microbial metabolic efficiency. *Nature Communications*, *9*, 3951. https://doi.org/10.1038/s41467-018-06232-y

Chen, R., Senbayram, M., Blagodatsky, S., Myachina, O., Dittert, K., Lin, X., … Kuzyakov, Y. (2014). Soil C and N availability determine the priming effect: Microbial N mining and stoichiometric decomposition theories. *Global Change Biology*, *20*, 2356–2367. https://doi.org/10.1111/gcb.12475

Cheng, W. (1996). Measurement of rhizosphere respiration and organic matter decomposition using natural 13C. *Plant and Soil*, *183*, 263–268. https://doi.org/10.1007/BF00011441

Cheng, W., & Dijkstra, F. A. (2007). Theoretical proof and empirical confirmation of a continuous labeling method using naturally 13C-depleted carbon dioxide. *Journal of Integrative Plant Biology*, *49*, 401–407.

Cheng, W., Johnson, D. W., & Fu, S. (2003). Rhizosphere effects on decomposition: controls of plant species, phenology, and fertilization. *Soil Science Society of America Journal*, *67*, 1418–1427. https://doi.org/10.2136/sssaj2003.1418

Cheng, W. X., & Kuzyakov, Y. (2005). Root effects on soil organic matter decomposition. In R. W. Zobel & S. F. Wright (Eds.), *Roots and soil management: Interactions between roots and the soil* (pp. 119–143). Madison, WI: American Society of Agronomy, Crop Science Society of America, Soil Science Society of America.

Cheng, W., Parton, W. J., Gonzalez-Meler, M. A., Phillips, R., Asao, S., McNickle, G. G., … Jastrow, J. D. (2014). Synthesis and modeling perspectives of rhizosphere priming. *New Phytologist*, *201*, 31–44. https://doi.org/10.1111/nph.12440

R Core Team. (2017). *R: A language and environment for statistical computing*. Vienna, Austria: R Foundation for Statistical Computing.

Cornwell, W. K., Cornelissen, J. H. C., Amatangelo, K., Dorrepaal, E., Eviner, V. T., Godoy, O., … Westoby, M. (2008). Plant species traits are the predominant control on litter decomposition rates within biomes worldwide. *Ecology Letters*, *11*, 1065–1071. https://doi.org/10.1111/j.1461-0248.2008.01219.x

Cotrufo, M. F., Soong, J. L., Horton, A. J., Campbell, E. E., Haddix, M. L., Wall, D. H., & Parton, W. J. (2015). Formation of soil organic matter via biochemical and physical pathways of litter mass loss. *Nature Geoscience*, *8*, 776–779. https://doi.org/10.1038/ngeo2520

Cotrufo, M. F., Wallenstein, M. D., Boot, C. M., Denef, K., & Paul, E. (2013). The Microbial Efficiency-Matrix Stabilization (MEMS) framework integrates plant litter decomposition with soil organic matter stabilization: Do labile plant inputs form stable soil organic matter? *Global Change Biology*, *19*, 988–995. https://doi.org/10.1111/gcb.12113

Craine, J. M., Wedin, D. A., & Chapin, F. S. (1999). Predominance of ecophysiological controls on soil CO_2 flux in a Minnesota grassland. *Plant and Soil*, *207*, 77–86.

Cros, C., Alvarez, G., Keuper, F., & Fontaine, S. (2019). A new experimental platform connecting the rhizosphere priming effect with CO_2 fluxes of plant-soil systems. *Soil Biology and Biochemistry*, *130*, 12–22. https://doi.org/10.1016/j.soilbio.2018.11.022

De Deyn, G. B., Cornelissen, J. H. C., & Bardgett, R. D. (2008). Plant functional traits and soil carbon sequestration in contrasting biomes. *Ecology Letters*, *11*, 516–531. https://doi.org/10.1111/j.1461-0248.2008.01164.x

Diaz, S., & Cabido, M. (2001). Vive la difference: Plant functional diversity matters to ecosystem processes. *Trends in Ecology & Evolution*, *16*, 646–655.

Dijkstra, F. A., Bader, N. E., Johnson, D. W., & Cheng, W. (2009). Does accelerated soil organic matter decomposition in the presence of plants increase plant N availability? *Soil Biology and Biochemistry*, *41*, 1080–1087. https://doi.org/10.1016/j.soilbio.2009.02.013

Dijkstra, F. A., & Cheng, W. (2007). Interactions between soil and tree roots accelerate long-term soil carbon decomposition. *Ecology Letters*, *10*, 1046–1053. https://doi.org/10.1111/j.1461-0248.2007.01095.x

Drake, J. E., Darby, B. A., Giasson, M. A., Kramer, M. A., Phillips, R. P., & Finzi, A. C. (2013). Stoichiometry constrains microbial response to root exudation- insights from a model and a field experiment in a temperate forest. *Biogeosciences*, *10*, 821–838. https://doi.org/10.5194/bg-10-821-2013

Farquhar, G. D., Ehleringer, J. R., & Hubick, K. T. (1989). Carbon isotope discrimination and photosynthesis. *Annual Review of Plant Physiology and Plant Molecular Biology*, *40*, 503–537. https://doi.org/10.1146/annurev.pp.40.060189.002443

Farrar, J., Hawes, M., Jones, D., & Lindow, S. (2003). How roots control the flux of carbon to the rhizosphere. *Ecology*, *84*, 827–837. https://doi.org/10.1890/0012-9658(2003)084[0827:HRCTFO]2.0.CO;2

Finzi, A. C., Abramoff, R. Z., Spiller, K. S., Brzostek, E. R., Darby, B. A., Kramer, M. A., & Phillips, R. P. (2015). Rhizosphere processes are quantitatively important components of terrestrial carbon and nutrient cycles. *Global Change Biology*, *21*, 2082–2094. https://doi.org/10.1111/gcb.12816

Fontaine, S., Barot, S., Barre, P., Bdioui, N., Mary, B., & Rumpel, C. (2007). Stability of organic carbon in deep soil layers controlled by fresh carbon supply. *Nature*, *450*, 277–U10. https://doi.org/10.1038/nature06275

Fontaine, S., Henault, C., Aamor, A., Bdioui, N., Bloor, J. M. G., Maire, V., … Maron, P. A. (2011). Fungi mediate long term sequestration of carbon and nitrogen in soil through their priming effect. *Soil Biology & Biochemistry*, *43*, 86–96. https://doi.org/10.1016/j.soilbio.2010.09.017

Fortunel, C., Garnier, E., Joffre, R., Kazakou, E., Quested, H., Grigulis, K., … Zarovali, M. (2009). Leaf traits capture the effects of land use changes and climate on litter decomposability of grasslands across Europe. *Ecology*, *90*, 598–611. https://doi.org/10.1890/08-0418.1

Freschet, G. T., Aerts, R., & Cornelissen, J. H. C. (2012). A plant economics spectrum of litter decomposability. *Functional Ecology*, *26*, 56–65. https://doi.org/10.1111/j.1365-2435.2011.01913.x

Freschet, G. T., Cornelissen, J. H. C., Van Logtestijn, R. S. P., & Aerts, R. (2010). Evidence of the 'plant economics spectrum' in a subarctic flora. *Journal of Ecology*, *98*, 362–373. https://doi.org/10.1111/j.1365-2745.2009.01615.x

Freschet, G. T., & Roumet, C. (2017). Sampling roots to capture plant and soil functions. *Functional Ecology*, *31*, 1506–1518. https://doi.org/10.1111/1365-2435.12883

Freschet, G. T., Valverde-Barrantes, O. J., Tucker, C. M., Craine, J. M., McCormack, M. L., Violle, C., … Roumet, C. (2017). Climate, soil and plant functional types as drivers of global fine-root trait variation. *Journal of Ecology*, *105*, 1182–1196. https://doi.org/10.1111/1365-2745.12769

Garnier, E., Cortez, J., Billès, G., Navas, M.-L., Roumet, C., Debussche, M., … Toussaint, J.-P. (2004). Plant functional markers capture ecosystem properties during secondary succession. *Ecology*, *85*, 2630–2637. https://doi.org/10.1890/03-0799

Grigulis, K., Lavorel, S., Krainer, U., Legay, N., Baxendale, C., Dumont, M., … Clément, J.-C. (2013). Relative contributions of plant traits and soil microbial properties to mountain grassland ecosystem services. *Journal of Ecology*, *101*, 47–57. https://doi.org/10.1111/1365-2745.12014

Guyonnet, J. P., Cantarel, A. A. M., Simon, L., Haichar, F. e. Z. (2018). Root exudation rate as functional trait involved in plant nutrient-use strategy classification. *Ecology and Evolution*, *8*, 8573–8581. https://doi.org/10.1002/ece3.4383

Heath, J., Ayres, E., Possell, M., Bardgett, R. D., Black, H. I. J., Grant, H., … Kerstiens, G. (2005). Rising atmospheric CO_2 reduces sequestration of root-derived soil carbon. *Science*, *309*, 1711–1713. https://doi.org/10.1126/science.1110700

Heimann, M., & Reichstein, M. (2008). Terrestrial ecosystem carbon dynamics and climate feedbacks. *Nature*, *451*, 289–292. https://doi.org/10.1038/nature06591

Högberg, P., & Read, D. J. (2006). Towards a more plant physiological perspective on soil ecology. *Trends in Ecology & Evolution*, *21*, 548–554. https://doi.org/10.1016/j.tree.2006.06.004

Henneron, L., Cros, C., Picon-Cochard, C., Rahimian, V., & Fontaine, S. (2019). Data from: Plant economic strategies of grassland species control soil carbon dynamics through rhizodeposition. *Dryad Digital Repository*, https://doi.org/10.5061/dryad.040jp22.

Huo, C., Luo, Y., & Cheng, W. (2017). Rhizosphere priming effect: A meta-analysis. *Soil Biology and Biochemistry*, *111*, 78–84. https://doi.org/10.1016/j.soilbio.2017.04.003

Joergensen, R. G. (1996). The fumigation-extraction method to estimate soil microbial biomass: Calibration of the kEC value. *Soil Biology and Biochemistry*, *28*, 25–31. https://doi.org/10.1016/0038-0717(95)00102-6

Johnson, D., Leake, J. R., Ostle, N., Ineson, P., & Read, D. J. (2002). In situ13CO_2 pulse-labelling of upland grassland demonstrates a rapid pathway of carbon flux from arbuscular mycorrhizal mycelia to the soil. *New Phytologist*, *153*, 327–334. https://doi.org/10.1046/j.0028-646X.2001.00316.x

Jones, D. L., Hodge, A., & Kuzyakov, Y. (2004). Plant and mycorrhizal regulation of rhizodeposition. *New Phytologist*, *163*, 459–480. https://doi.org/10.1111/j.1469-8137.2004.01130.x

Jones, D. L., Nguyen, C., & Finlay, R. D. (2009). Carbon flow in the rhizosphere: Carbon trading at the soil–root interface. *Plant and Soil*, *321*, 5–33. https://doi.org/10.1007/s11104-009-9925-0

Kallenbach, C. M., Frey, S. D., & Grandy, A. S. (2016). Direct evidence for microbial-derived soil organic matter formation and its ecophysiological controls. *Nature Communications*, *7*, 13630. https://doi.org/10.1038/ncomms13630

Keiluweit, M., Bougoure, J. J., Nico, P. S., Pett-Ridge, J., Weber, P. K., & Kleber, M. (2015). Mineral protection of soil carbon counteracted by root exudates. *Nature Clim. Change*, *5*, 588–595.

Klumpp, K., Fontaine, S., Attard, E., Le Roux, X., Gleixner, G., & Soussana, J.-F. (2009). Grazing triggers soil carbon loss by altering plant roots and their control on soil microbial community. *Journal of Ecology*, *97*, 876–885. https://doi.org/10.1111/j.1365-2745.2009.01549.x

Klumpp, K., Soussana, J. F., & Falcimagne, R. (2007). Effects of past and current disturbance on carbon cycling in grassland mesocosms. *Agriculture, Ecosystems & Environment*, *121*, 59–73. https://doi.org/10.1016/j.agee.2006.12.005

Kramer-Walter, K. R., Bellingham, P. J., Millar, T. R., Smissen, R. D., Richardson, S. J., & Laughlin, D. C. (2016). Root traits are multidimensional: Specific root length is independent from root tissue density and the plant economic spectrum. *Journal of Ecology*, *104*, 1299–1310. https://doi.org/10.1111/1365-2745.12562

Kuzyakov, Y. (2002). Review: Factors affecting rhizosphere priming effects. *Journal of Plant Nutrition and Soil Science*, *165*, 382–396. https://doi.org/10.1002/1522-2624(200208)165:4<382:AID-JPLN382>3.0.CO;2-#

Kuzyakov, Y., & Cheng, W. (2001). Photosynthesis controls of rhizosphere respiration and organic matter decomposition. *Soil Biology and Biochemistry*, *33*, 1915–1925. https://doi.org/10.1016/S0038-0717(01)00117-1

Kuzyakov, Y., & Gavrichkova, O. (2010). Time lag between photosynthesis and carbon dioxide efflux from soil: A review of mechanisms and controls. *Global Change Biology*, *16*, 3386–3406.

Laliberté, E. (2017). Below-ground frontiers in trait-based plant ecology. *New Phytologist*, *213*, 1597–1603. https://doi.org/10.1111/nph.14247

Lambers, H., & Poorter, H. (1992). Inherent variation in growth rate between higher plants: A search for physiological causes and ecological consequences. In M. Begon & A. H. Fitter (Eds.), *Advances in ecological research* (pp. 187–261). Cambridge, UK: Academic Press.

Liang, C., Schimel, J. P., & Jastrow, J. D. (2017). The importance of anabolism in microbial control over soil carbon storage. *Nature Microbiology*, *2*, 17105. https://doi.org/10.1038/nmicrobiol.2017.105

Louault, F., Pillar, V., Aufrere, J., Garnier, E., & Soussana, J.-F. (2005). Plant traits and functional types in response to reduced disturbance in a semi-natural grassland. *Journal of Vegetation Science*, *16*, 151–160. https://doi.org/10.1111/j.1654-1103.2005.tb02350.x

Luo, Y., Ahlström, A., Allison, S. D., Batjes, N. H., Brovkin, V., Carvalhais, N., … Zhou, T. (2016). Toward more realistic projections of soil carbon dynamics by Earth system models. *Global Biogeochemical Cycles*, *30*, 40–56. https://doi.org/10.1002/2015GB005239

Ma, Z., Guo, D., Xu, X., Lu, M., Bardgett, R. D., Eissenstat, D. M., … Hedin, L. O. (2018). Evolutionary history resolves global organization of root functional traits. *Nature*, *555*, 94. https://doi.org/10.1038/nature25783

Meier, U. (2003). Phenological growth stages. In M. D. Schwartz (Ed.), *Phenology: An integrative environmental science* (pp. 269–283). Dordrecht, The Netherlands: Springer.

Miltner, A., Bombach, P., Schmidt-Brücken, B., & Kästner, M. (2012). SOM genesis: Microbial biomass as a significant source. *Biogeochemistry*, *112*, 41–45. https://doi.org/10.1007/s10533-011-9658-z

Nolan, C., Overpeck, J. T., Allen, J. R. M., Anderson, P. M., Betancourt, J. L., Binney, H. A., … Jackson, S. T. (2018). Past and future global transformation of terrestrial ecosystems under climate change. *Science*, *361*, 920–923. https://doi.org/10.1126/science.aan5360

Orwin, K. H., Buckland, S. M., Johnson, D., Turner, B. L., Smart, S., Oakley, S., & Bardgett, R. D. (2010). Linkages of plant traits to soil properties and the functioning of temperate grassland. *Journal of Ecology*, *98*, 1074–1083. https://doi.org/10.1111/j.1365-2745.2010.01679.x

Pascault, N., Ranjard, L., Kaisermann, A., Bachar, D., Christen, R., Terrat, S., … Maron, P.-A. (2013). Stimulation of different functional groups of bacteria by various plant residues as a driver of soil priming effect. *Ecosystems*, *16*, 810–822. https://doi.org/10.1007/s10021-013-9650-7

Pausch, J., & Kuzyakov, Y. (2018). Carbon input by roots into the soil: Quantification of rhizodeposition from root to ecosystem scale. *Global Change Biology*, *24*, 1–12. https://doi.org/10.1111/gcb.13850

Personeni, E., & Loiseau, P. (2004). How does the nature of living and dead roots affect the residence time of carbon in the root litter continuum? *Plant and Soil*, *267*, 129–141. https://doi.org/10.1007/s11104-005-4656-3

Perveen, N., Barot, S., Alvarez, G., Klumpp, K., Martin, R., Rapaport, A., … Fontaine, S. (2014). Priming effect and microbial diversity in ecosystem functioning and response to global change: A modeling approach using the SYMPHONY model. *Global Change Biology*, *20*, 1174–1190. https://doi.org/10.1111/gcb.12493

Phillips, R. P., Meier, I. C., Bernhardt, E. S., Grandy, A. S., Wickings, K., & Finzi, A. C. (2012). Roots and fungi accelerate carbon and nitrogen cycling in forests exposed to elevated CO_2. *Ecology Letters*, *15*, 1042–1049.

Poorter, H., Niklas, K. J., Reich, P. B., Oleksyn, J., Poot, P., & Mommer, L. (2012). Biomass allocation to leaves, stems and roots: Meta-analyses of interspecific variation and environmental control. *New Phytologist*, *193*, 30–50. https://doi.org/10.1111/j.1469-8137.2011.03952.x

Prieto, I., Roumet, C., Cardinael, R., Dupraz, C., Jourdan, C., Kim, J. H., … Stokes, A. (2015). Root functional parameters along a land-use gradient: Evidence of a community-level economics spectrum. *Journal of Ecology*, *103*, 361–373. https://doi.org/10.1111/1365-2745.12351

Quested, H., Eriksson, O., Fortunel, C., & Garnier, E. (2007). Plant traits relate to whole-community litter quality and decomposition following land use change. *Functional Ecology*, *21*, 1016–1026. https://doi.org/10.1111/j.1365-2435.2007.01324.x

Rasse, D. P., Rumpel, C., & Dignac, M.-F. (2005). Is soil carbon mostly root carbon? Mechanisms for a specific stabilisation. *Plant and Soil*, *269*, 341–356. https://doi.org/10.1007/s11104-004-0907-y

Reich, P. B. (2014). The world-wide 'fast–slow' plant economics spectrum: A traits manifesto. *Journal of Ecology*, *102*, 275–301. https://doi.org/10.1111/1365-2745.12211

Reich, P. B., Buschena, C., Tjoelker, M. G., Wrage, K., Knops, J., Tilman, D., & Machado, J. L. (2003). Variation in growth rate and ecophysiology among 34 grassland and savanna species under contrasting N supply: A test of functional group differences. *New Phytologist*, *157*, 617–631. https://doi.org/10.1046/j.1469-8137.2003.00703.x

Roumet, C., Birouste, M., Picon-Cochard, C., Ghestem, M., Osman, N., Vrignon-Brenas, S., … Stokes, A. (2016). Root structure–function relationships in 74 species: Evidence of a root economics spectrum related to carbon economy. *New Phytologist*, *210*, 815–826. https://doi.org/10.1111/nph.13828

Schimel, J., & Schaeffer, S. M. (2012). Microbial control over carbon cycling in soil. *Frontiers in Microbiology*, *3*, https://doi.org/10.3389/fmicb.2012.00348

Schlesinger, W. H., & Bernhardt, E. S. (2013). *Biogeochemistry: An analysis of global change*. Boston, MA: Academic Press.

Schmidt, M. W. I., Torn, M. S., Abiven, S., Dittmar, T., Guggenberger, G., Janssens, I. A., … Trumbore, S. E. (2011). Persistence of soil organic matter as an ecosystem property. *Nature*, *478*, 49–56. https://doi.org/10.1038/nature10386

Schnyder, H., & Lattanzi, F. A. (2005). Partitioning respiration of C3–C4 mixed communities using the natural abundance 13C approach – Testing assumptions in a controlled environment. *Plant Biology*, *7*, 592–600.

Shahzad, T., Chenu, C., Genet, P., Barot, S., Perveen, N., Mougin, C., & Fontaine, S. (2015). Contribution of exudates, arbuscular mycorrhizal fungi and litter depositions to the rhizosphere priming effect induced by grassland species. *Soil Biology and Biochemistry*, *80*, 146–155. https://doi.org/10.1016/j.soilbio.2014.09.023

Shahzad, T., Chenu, C., Repinçay, C., Mougin, C., Ollier, J.-L., & Fontaine, S. (2012). Plant clipping decelerates the mineralization of recalcitrant soil organic matter under multiple grassland species. *Soil Biology and Biochemistry*, *51*, 73–80. https://doi.org/10.1016/j.soilbio.2012.04.014

Sinsabaugh, R. L., Moorhead, D. L., Xu, X., & Litvak, M. E. (2017). Plant, microbial and ecosystem carbon use efficiencies interact to stabilize microbial growth as a fraction of gross primary production. *New Phytologist*, *214*, 1518–1526. https://doi.org/10.1111/nph.14485

Sokol, N. W., Kuebbing, S. E., Karlsen-Ayala, E., & Bradford, M. A. (2018). Evidence for the primacy of living root inputs, not root or shoot litter, in forming soil organic carbon. *New Phytologist*, *221*, 233–246. https://doi.org/10.1111/nph.15361

van Groenigen, K. J., Osenberg, C. W., Terrer, C., Carrillo, Y., Dijkstra, F. A., Heath, J., … Hungate, B. A. (2017). Faster turnover of new soil carbon inputs under increased atmospheric CO_2. *Global Change Biology*, *23*, 4420–4429.

Vance, E. D., Brookes, P. C., & Jenkinson, D. S. (1987). An extraction method for measuring soil microbial biomass C. *Soil Biology & Biochemistry*, *19*, 703–707. https://doi.org/10.1016/0038-0717(87)90052-6

Vitousek, P. M., & Howarth, R. W. (1991). Nitrogen limitation on land and in the sea: How can it occur? *Biogeochemistry*, *13*, 87–115. https://doi.org/10.1007/BF00002772

Wang, X., Tang, C., Severi, J., Butterly, C. R., & Baldock, J. A. (2016). Rhizosphere priming effect on soil organic carbon decomposition under plant species differing in soil acidification and root exudation. *New Phytologist*, *211*, 864–873. https://doi.org/10.1111/nph.13966

Wardle, D. A., Bardgett, D. G., Klironomos, J. N., Setälä, H., van der Putten, W. H., & Wall, D. H. (2004). Ecological linkages between aboveground and belowground biota. *Science*, *304*, 1629–1633. https://doi.org/10.1126/science.1094875

Warembourg, F. R., Roumet, C., & Lafont, F. (2003). Differences in rhizosphere carbon-partitioning among plant species of different families. *Plant and Soil*, *256*, 347–357.

Weemstra, M., Mommer, L., Visser, E. J. W., van Ruijven, J., Kuyper, T. W., Mohren, G. M. J., & Sterck, F. J. (2016). Towards a multidimensional root trait framework: A tree root review. *New Phytologist*, *211*, 1159–1169. https://doi.org/10.1111/nph.14003

Werth, M., & Kuzyakov, Y. (2010). 13C fractionation at the root–microorganisms–soil interface: A review and outlook for partitioning studies. *Soil Biology and Biochemistry*, *42*, 1372–1384. https://doi.org/10.1016/j.soilbio.2010.04.009

Wright, I. J., Reich, P. B., Westoby, M., Ackerly, D. D., Baruch, Z., Bongers, F., … Villar, R. (2004). The worldwide leaf economics spectrum. *Nature*, *428*, 821–827. https://doi.org/10.1038/nature02403

Yin, L., Dijkstra Feike, A., Wang, P., Zhu, B., & Cheng, W. (2018). Rhizosphere priming effects on soil carbon and nitrogen dynamics among tree species with and without intraspecific competition. *New Phytologist*, *218*, 1036–1048. https://doi.org/10.1111/nph.15074

SUPPORTING INFORMATION

Additional supporting information may be found online in the Supporting Information section at the end of the article.

How to cite this article: Henneron L, Cros C, Picon-Cochard C, Rahimian V, Fontaine S. Plant economic strategies of grassland species control soil carbon dynamics through rhizodeposition. *J Ecol*. 2020;108:528–545. https://doi.org/10.1111/1365-2745.13276